JACS
JOURNAL OF THE AMERICAN CHEMICAL SOCIETY
pubs.acs.org/JACS
Article

Asymmetric [4 + 2], [6 + 2], and [6 + 4] Cycloadditions of Isomeric Formyl Cycloheptatrienes Catalyzed by a Chiral Diamine Catalyst

Mikk Kaasik,[#] Pan-Pan Chen,[#] Sebastijan Ričko, Karl Anker Jørgensen,* and K. N. Houk*

Cite This: J. Am. Chem. Soc. 2023, 145, 23874−23890
Read Online
ACCESS | Metrics & More | Article Recommendations | Supporting Information

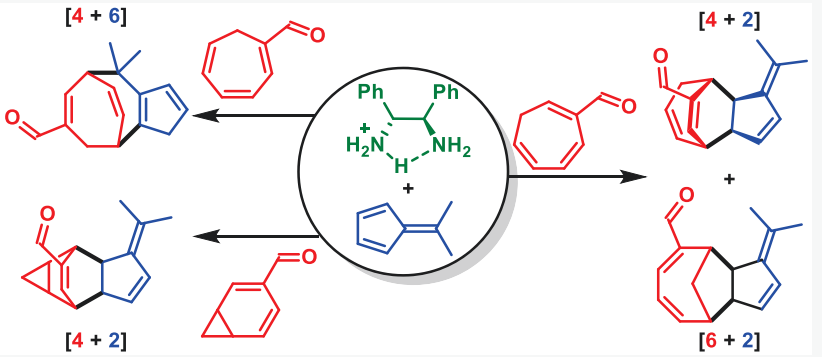

ABSTRACT: Novel asymmetric aminocatalytic cycloadditions are described between formyl cycloheptatrienes and 6,6-dimethylfulvene that lead to [4 + 2], [6 + 2], and [4 + 6] cycloadducts. The unprecedented reaction course is dependent on the position of the formyl functionality in the cycloheptatriene core, and each formyl cycloheptatriene isomer displays a distinct reactivity pattern. The formyl cycloheptatriene isomers are activated by a chiral primary diamine catalyst, and the activation mode is dependent on the position of the formyl functionality relative to the cycloheptatriene core. The [4 + 2] and [6 + 2] cycloadducts are formed via rare iminocatalytic inverse electron-demand cycloadditions, while the [4 + 6] cycloadduct is formed by a normal electron-demand cycloaddition. The reactivity displayed by the different formyl cycloheptatrienes was investigated by DFT calculations. These computational studies account for the different reaction paths for the three isomeric formyl cycloheptatrienes. The aminocatalytic [4 + 2], [6 + 2], and [4 + 6] cycloadditions proceed by stepwise processes, and the interplay between conjugation, substrate distortion, and dispersive interactions between the fulvene and aminocatalyst mainly defines the outcome of each cycloaddition.

INTRODUCTION

Polyenes play an important role in asymmetric synthesis as they can be applied to generate complex molecular scaffolds, especially if challenges related to peri-, chemo-, diastereo-, and enantioselectivity can be resolved.[1,2] Cycloheptatriene and its derivatives have received widespread attention due to the pericyclic reactions they can undergo.[3,4] Furthermore, the structural core element is also part of bioactive compounds.[5−7]

Cycloheptatriene reacts with, for example, cyclopentadiene at elevated temperatures with formation of different cycloadducts, including cycloadducts from cyclopentadiene self-reactions, and cycloheptatriene dimerization.[8−10] Recent studies of the dimerization of cycloheptatriene have elucidated a complex reaction profile. At 200 °C a concerted [6 + 4] cycloaddition proceeds via an ambimodal [6 + 4]/[4 + 6] transition state. By increasing the reaction temperature to 300 °C, a competing stepwise diradical [6 + 2] cycloaddition takes place (Scheme 1a).[11] The reactions of cycloheptatrienes can also be promoted by using metal catalysis. However, this too does not always preclude the use of elevated temperatures, which can hinder the use of more labile substrates.[12,13]

The cycloheptatriene core can be activated by the introduction of various functionalities. Thus, the introduction of these functionalities will make the cycloheptatriene core more accessible for cycloadditions; but on the other hand, these can additionally increase the number of competing reaction paths. To exemplify this, cycloheptatrienes can undergo substituent-dependent photochemical rearrangements or electrocyclizations, resulting in their isomers or bicyclo[3.2.0]hepta-2,6-dienes, respectively (Scheme 1b).[14] Furthermore, in the ground state, an equilibrium exists between the cycloheptatriene and its norcaradiene isomer (Scheme 1c). The equilibrium is generally

Received: August 31, 2023
Published: October 20, 2023

https://doi.org/10.1021/jacs.3c09551
J. Am. Chem. Soc. 2023, 145, 23874−23890

Scheme 1. (a) Thermal Dimerization of Cycloheptatriene; (b) Excited State Reactivity of Substituted Cycloheptatrienes; (c) Competing Thermal [4 + 2] Cycloadditions of Substituted Cycloheptatrienes

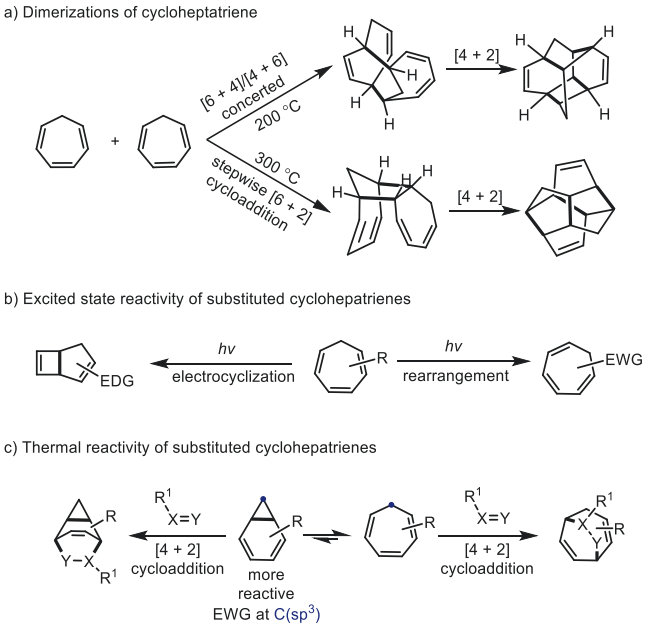

shifted toward the former, but it can be altered by variation of substituents on the cycloheptatriene.[15−17] This valence isomerism has intrigued chemists for over 50 years.[18,19] As cycloadditions can proceed through either isomer, cycloadditions have been one of the primary means to explore this equilibrium.[20] Generally, the norcaradiene is more reactive than the cycloheptatriene isomer, and this can be further amplified, for example, with the addition of electron-withdrawing substituents on the sp^3-carbon atom of the cycloheptatriene isomer.[21]

Substituents can also be used as handles to activate the cycloheptatriene core through catalysis in normal and higher-order cycloadditions.[22−25] While heptafulvenes and tropones have been shown to undergo different enantioselective cycloadditions, these molecules are seldom used for reaction control,[26−30] which is generally achieved through the other cycloaddend.[31−40] To this end, formyl-substituted cycloheptatrienes could serve as promising model substrates, as the formyl group can both activate the system and potentially enable reaction control using, for example, asymmetric aminocatalysis.[41,42] Despite this, formyl-substituted cycloheptatrienes have found limited use, which may be in part due to the difficulty in controlling their reactivity.[43−45]

To advance the application of formyl-substituted cycloheptatrienes in organic synthesis, we investigated their reactivity in cycloaddition reactions with 6,6-dimethylfulvene applying aminocatalytic conditions. The reaction concept for aminocatalytic activation of isomeric formyl cycloheptatrienes is based on the LUMO-lowering strategy (Scheme 2a), as a HOMO-raising strategy of, for example, cyclohepta-1,3,5-triene-1-carbaldehyde **1** will generate an *anti*-aromatic intermediate (Scheme 2b). The LUMO-lowering strategy requires the generation of an iminium ion or imine intermediate, which can be achieved with a secondary or primary amine catalyst, respectively. Iminium catalysis has been one of the cornerstones of asymmetric organocatalysis since the ground-breaking disclosure by MacMillan et al. in 2000.[46] Over the years, iminium catalysis has been successfully used to carry out a range of cycloaddition and cyclization reactions.[47−49] Contrary to these varied examples, iminium catalysis has not gained as much success regarding asymmetric higher-order cycloadditions, for which only a few examples have been disclosed.[39,50]

By applying aminocatalysis for the LUMO-activation of isomeric formyl cycloheptatrienes, the three formyl cycloheptatrienes **1**−**3**, along with their norcaradiene isomers **N1**−**N3** (Scheme 3a), can participate in a number of cycloadditions, as several distinct 2π-, 4π-, or 6π-addends can be envisioned. For formyl cycloheptatriene **1**, nine different π-addends are possible (Scheme 3b), and the same also applies for cyclohepta-1,4,6-triene-1-carbaldehyde **2** and cyclohepta-1,3,6-triene-1-carbaldehyde **3** (*vide infra*). 6,6-Dimethylfulvene **4** can also act as a 2π- (for a nonsymmetric fulvene, the two olefins in the ring will be different), 4π-, or 6π-addend (Scheme 3c); therefore, numerous cycloadducts can form by the reaction of formyl cycloheptatrienes **1**−**3** with fulvene **4**.

We have found that each isomeric formyl cycloheptatriene **1**−**3** reacts differently with fulvene **4** in the presence of chiral diamine aminocatalyst **I** (Scheme 4). Formyl cycloheptatriene **1** reacts as a 4π-addend in a [4 + 6] cycloaddition, and formyl cycloheptatriene **2** acts primarily as a 4π-addend in a [4 + 2] cycloaddition, the major reaction pathway, and secondarily as a 6π-addend in a [6 + 2] cycloaddition, the minor reaction pathway. The 3-formyl cycloheptatriene **3** participates as a 4π-addend through its norcaradiene isomer **N3** in a [4 + 2] cycloaddition (Scheme 3).

Interestingly, as LUMO-activated formyl cycloheptatrienes **2** and **3** contribute more π-bonds than fulvene **4** to the

Scheme 2. Aminocatalytic Activation of Formyl Cycloheptatriene 1: (a) LUMO-Activation and (b) HOMO-Activation

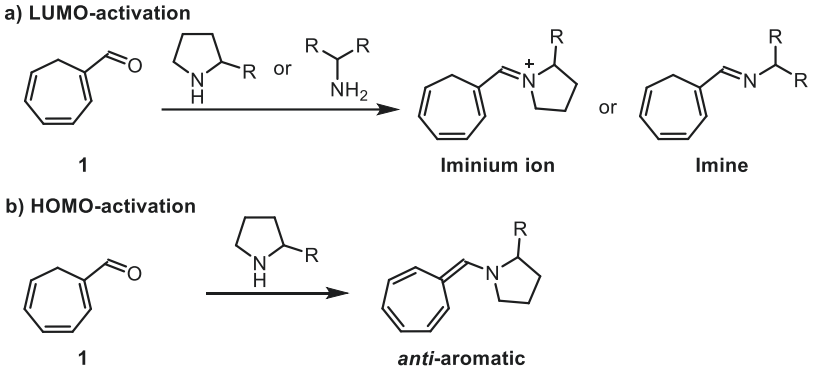

https://doi.org/10.1021/jacs.3c09551
J. Am. Chem. Soc. 2023, 145, 23874−23890

Scheme 3. Possible *nπ*-Addends for Formyl Cycloheptatriene 1 and Fulvene 4

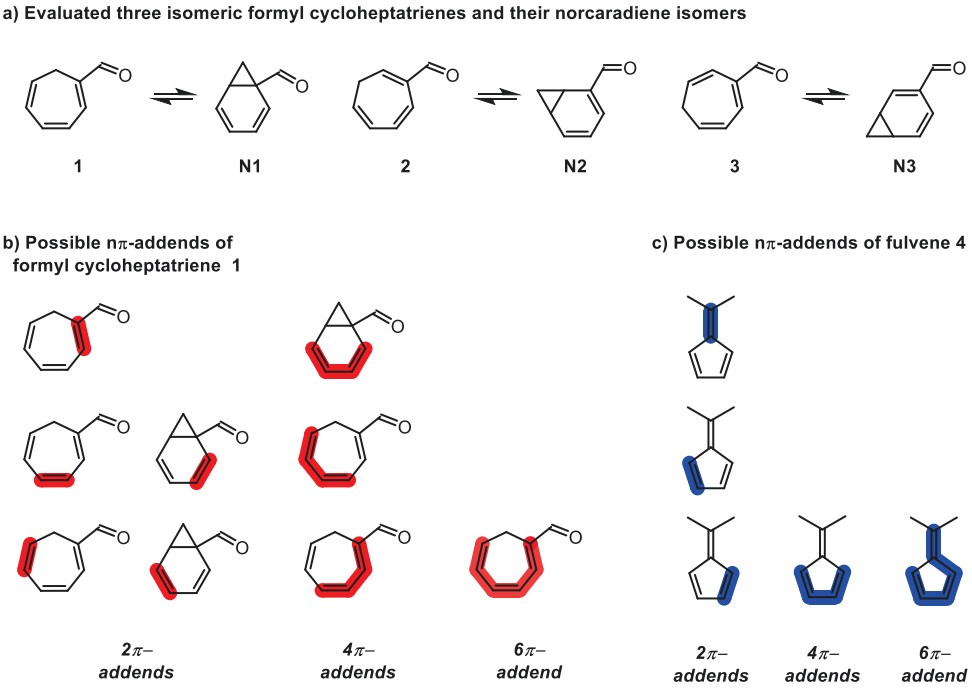

Scheme 4. Observed Cycloadditions for Reactions of Isomeric Formyl Cycloheptarienes 1−3 with Fulvene 4 in the Presence of Aminocatalyst (1*R*,2*R*)-1,2-Diphenylethane-1,2-diamine (I)

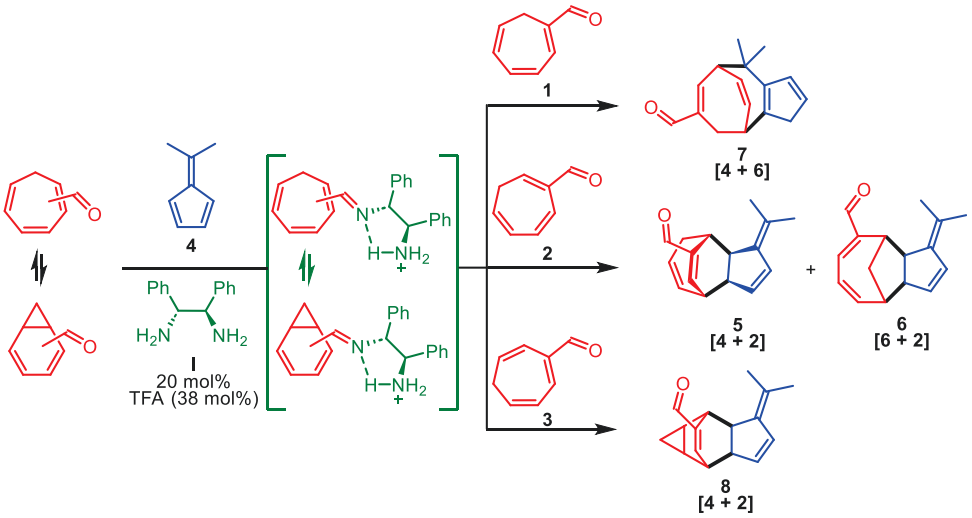

cycloaddition, the reactions leading to cycloadducts **5**, **6**, and **8** are inverse electron-demand cycloadditions. Activation of conjugated systems, such as the one present in formyl cycloheptatrienes, applying the enantioselective iminocatalytic inverse electron-demand strategy is rare[51] and has been mainly described for Lewis acid activation.[26,27,52,53] More precisely, iminium catalytic inverse electron-demand Diels−Alder reactions are, to the best of our knowledge, unprecedented.

We describe how introducing a formyl substituent to the cycloheptatriene system, combined with aminocatalysis, allows for a novel approach to exert control of periselectivity and reactivity in cycloadditions. The present work includes experimental and computational investigations addressing unprecedented reactivities governed by linear- versus cross-conjugated intermediates as well as a cycloaddition involving the cycloheptatriene−norcaradiene equilibrium. We anticipate that this study will increase the understanding of the reactivity of formyl cycloheptatrienes and stimulate the development of novel classes of cycloadditions, including asymmetric higher-order cycloadditions.[2,4]

RESULTS AND DISCUSSION

Initial Observations and Isomerization of Formyl Cycloheptatrienes. During an investigation of the reaction of formyl cycloheptatriene **1** with fulvene **4**, under combined amino- and photocatalytic conditions, we were surprised that the [4 + 2] and [6 + 2] inverse electron-demand cycloadducts, **5** and **6**, respectively, were formed, with **5** as the major cycloadduct (eq 1, see Supporting Information Table S2).

https://doi.org/10.1021/jacs.3c09551
J. Am. Chem. Soc. 2023, 145, 23874−23890

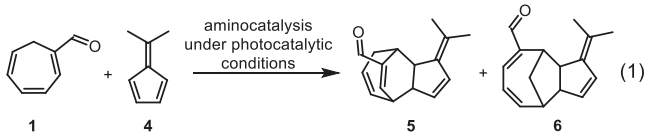

This outcome implies that formyl cycloheptatriene **2**, instead of **1**, reacted with fulvene **4**. The unexpected formation of **5** and **6** encouraged us initially to investigate the isomerization of formyl cycloheptatrienes **1**−**3** (Table 1).

Table 1. Studies of the Isomerization of Formyl Cycloheptatrienes 1−3 (See Supporting Information Table S1)

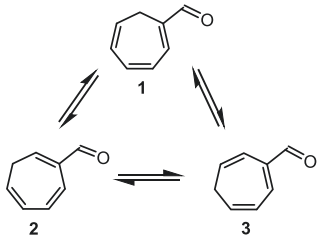

Entry	Starting compound	Energy source	Time	Product	Yield[a] [%]
1	**1**	Heat 120 °C	4 d	–	n.r.
2	**1**	400 nm LED	1.5 h	**2**	76
3	**2**	Heat 120 °C	3 d	–	n.r.
4	**2**	400 nm LED	6.5 h	–	n.r.
5	**3**	Heat 120 °C	3 d	–	–[b]
6	**3**	400 nm LED	6.5 h	–	n.r.

[a]Determined by ^{1}H NMR analysis of the reaction mixture and relative to the internal standard 1,3,5-tris(trifluoromethyl)benzene; n.r. = no reaction. [b]Decomposition of starting material.

It has been reported that formyl cycloheptatriene **2** can be synthesized from formyl cycloheptatriene **1** via a photoisomerization process utilizing a high-pressure Hg lamp with a Pyrex filter.[54] We found that this isomerization also proceeds using irradiation by fluorescent light bulbs or LEDs (Supporting Information Table S1). The best results were obtained by 400 nm LED irradiation as **1** was converted to **2**, along with some degree of polymerization of **1**, within 1.5 h (Table 1, entry 2). Next, formyl cycloheptatrienes **2** and **3** were irradiated with 400 nm LEDs. However, neither **2** nor **3** isomerized under these conditions (Table 1, entries 4 and 6). The three formyl cycloheptatrienes **1**−**3** could also be envisioned to interconvert between one another via a 1,5-hydrogen shift, or sequential 1,5-hydrogen shifts.[55] The possibility of thermal isomerization was also explored. However, even at 120 °C with a prolonged reaction time of 3 d, **1**, **2**, or **3** did not interconvert (Table 1, entries 1, 3, and 5). These results show that out of the three isomers, only **1** can be selectively converted to **2**, and only under photochemical conditions.

To obtain information about the isomerization between the three isomers of formyl cycloheptatrienes **1**−**3**, computational investigations were performed. The calculated results (see Supporting Information Figure S4) indicate that the proposed isomerization pathways, such as 1,5- or 1,7-hydrogen shifts, or tautomerization first and then alkyl migration, are not feasible under ordinary thermal conditions, consistent with the experimental observations. Photofacilitated polyene isomerization has been theoretically investigated previously.[56,57] This pathway is invoked for the isomerization of **1** to **2** based on the experimental observations and improbability of a thermal isomerization.

Aminocatalytic Cycloaddition of Formyl Cycloheptatriene 2 with Fulvene 4. Based on the results in Table 1, in which formyl cycloheptatriene **1** was converted to formyl cycloheptatriene **2** by a photoisomerization process, we started investigating the aminocatalytic reaction of **2** with fulvene **4** in the absence of light irradiation.

Table 2 presents the screening of different aminocatalysts for the reaction of **2** with **4**, where CH_2Cl_2 in the presence of trifluoroacetic acid (TFA) was chosen as the solvent as it gave satisfactory conversion and selectivity compared to toluene and MeCN (see Supporting Information Table S3). The screening revealed a significant preference for the [4 + 2] cycloadduct **5**. The results in Table 2 will focus on the [4 + 2] cycloaddition, and we will return to the [6 + 2] cycloaddition later.

Table 2. Screening of Aminocatalysts for the [4 + 2] Cycloaddition of Formyl Cycloheptatriene 2 with Fulvene 4

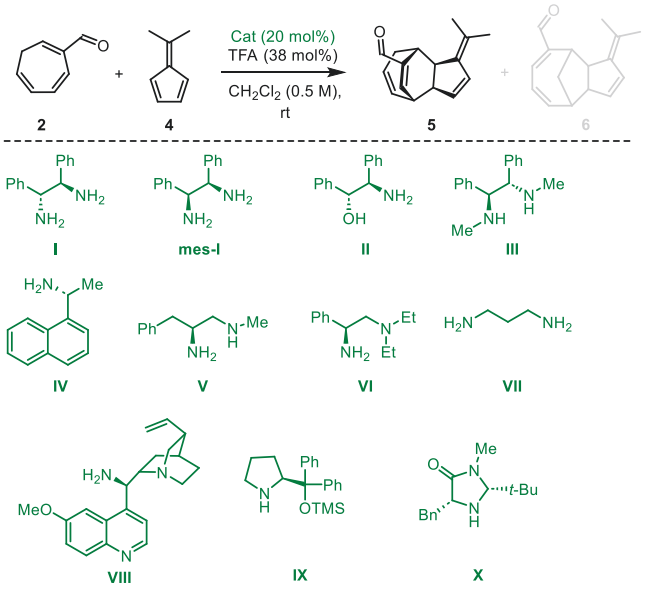

Entry	Catalyst	Time	NMR distribution [%][a] 2	5	ee [%][b]
1	**I**	20 h	3	65 (68)	89
2	mes-I	7 d	38	47	–
3[c]	**II**	7 d	52	23	17
4	**III**	20 d	77	1	–
5[c]	**IV**	7 d	62	12	−12
6	**V**	7 d	11	69 (70)	−73
7	**VI**	3 d	7	66 (52)	−65
8	**VII**	7 d	81	1	–
9[d]	**VIII**	7 d	89	4	–
10[c]	**IX**	7 d	72	–	–
11[c]	**X**	7 d	96	2	–

[a]Determined by ^{1}H NMR analysis of the reaction mixture and relative to the internal standard 1,3,5-tris(trifluoromethyl)benzene. Isolated yield in parentheses. [b]ee measured by UPC^2. [c]With 19 mol % TFA. [d]With 40 mol % of TFA.

Among the evaluated aminocatalysts, primary amines displayed higher conversions compared to secondary amines. (1*R*,2*R*)-1,2-Diphenylethane-1,2-diamine **I** gave the most promising result, providing **5** in 68% yield and 89% ee (Table 2, entry 1). No significant improvement in enantioselectivity was

https://doi.org/10.1021/jacs.3c09551
J. Am. Chem. Soc. 2023, 145, 23874−23890

found using the naphthyl analogue of **I** (see Supporting Information Table S4), while the *meso*-isomer of **I** was a less effective catalyst (Table 2, entry 2). The corresponding amino alcohol **II** was even less effective, affording **5** in only a 23% yield and 17% ee (Table 2, entry 3). Catalyst **III** (the dimethyl-substituted analogue of **I**) was ineffective, while (*R*)-1-(naphthalen-1-yl)ethan-1-amine **IV** afforded **5** in low yield and enantioselectivity (Table 2, entries 4 and 5). (*S*)-*N*1-Methyl-3-phenylpropane-1,2-diamine **V** delivered **5** in 70% yield and 73% ee (Table 2, entry 6). Similar results were obtained for catalyst **VI** (Table 2, entry 7). Other aminocatalysts and among them several typically used ones, such as **VII**–**X** (see Supporting Information Table S4), were ineffective (entries 8–11).

The formation of cycloadduct **5** was observed only with primary diamines **I**, **V**, and **VI**, while established chiral secondary amines were inactive. Related diamine systems have previously been used by Ishihara and Maruoka to address the issue of inactivity caused by A-1,3 strain, of secondary amines in Diels–Alder reactions of α-substituted enals.[58−61] It was postulated that primary aminocatalysts with an additional amino functionality could form the imine intermediate more readily and utilize intramolecular hydrogen bonding to enhance catalytic activity. Thus, acid additives were screened to investigate how acid influences the role of potential hydrogen bonding.

Table 3, entry 1 presents the results in the presence of TFA where the [4 + 2] cycloadduct **5** was obtained in 68% yield and

Table 3. Screening of Acids for the [4 + 2] Cycloaddition of Formyl Cycloheptatriene 2 with Fulvene 4 in the Presence of Aminocatalyst I

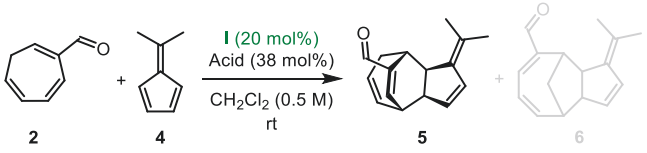

Entry	Acid (pK_a in MeCN)[a]	Time	NMR distribution [%][b] 2	5	ee [%][c]
1	TFA (12.7)	20 h	3	65 (68)	89
2	AcOH (23.5)	7 d	62	2	–
3	(−)-CSA	7 d	8	83	88
4	(+)-CSA	7 d	36	46	71
5	TCA (10.8)	20 h	2	85 (78)	93
6	TsOH (8.0)	7 d	70	20	–
7	TfOH (2.6)	20 h	40	–	–

[a]Experimental pK_a values reported; methanesulfonic acid has a pK_a value of 10.0, and we assume that CSA is in the same range.[62] [b]Determined by ^{1}H NMR analysis of the reaction mixture and relative to the internal standard 1,3,5-tris(trifluoromethyl)benzene. Isolated yield in parentheses. [c]ee measured by UPC^2.

89% ee. In contrast, only trace reactivity was observed after 1 week when changing to a weaker acid, such as acetic acid (Table 3, entry 2). Interestingly, a match/mismatch effect was observed using camphorsulfonic acid (CSA); (−)-CSA led to both higher conversion and enantioselectivity compared to the (+)-CSA (entries 3 and 4). Utilizing the slightly more acidic trichloroacetic acid (TCA) instead of TFA improved both the yield and enantioselectivity of **5** to 78% and 93% ee, respectively (Table 3, entry 5). The reaction became sluggish with stronger acids, for example, *p*-toluenesulfonic acid and TfOH (Table 3, entries 6 and 7). The data in Table 3 show that acids with pK_a values in the 10–13 range measured in MeCN are optimal for the [4 + 2] cycloaddition of formyl cycloheptatriene **2** with fulvene **4** in the presence of aminocatalyst **I**.

The absolute configuration of the [4 + 2] cycloadduct **5**, obtained using (1*R*,2*R*)-1,2-diphenylethane-1,2-diamine **I** as the aminocatalyst, was determined by single-crystal X-ray diffraction data for the hydrazone derivative of **5** (see Supporting Information Figure S3).

Throughout the screening experiments, particular attention was also paid to results that would lead to an increase in the conversion to [6 + 2] cycloadduct **6** (eq 2).

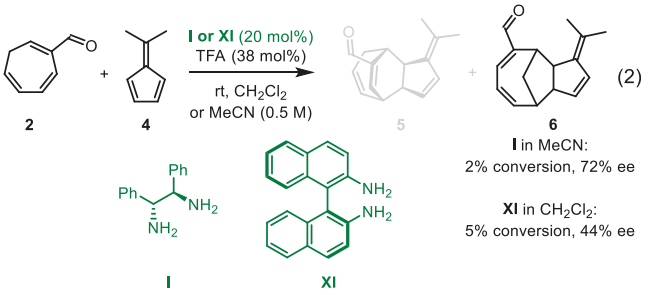

(2)

Unfortunately, we could not ascertain conditions that afforded [6 + 2] cycloadduct **6** in any meaningful quantities. In the presence of (1*R*,2*R*)-1,2-diphenylethane-1,2-diamine **I**, a conversion of 2% into cycloadduct **6** was observed only in MeCN. A slight improvement in conversion (5%) was obtained with [1,1′-binaphthalene]-2,2′-diamine **XI** as the catalyst (see Supporting Information Table S5). Cycloadduct **6** was formed with 72% ee and 44% ee, applying diamine catalysts **I** and **XI** showing that **6** is formed through an alternative minor aminocatalytic pathway and not through background reactivity.

Aminocatalytic Cycloaddition of Formyl Cycloheptatriene 1 with Fulvene 4. After elucidating the aminocatalytic cycloaddition of formyl cycloheptatriene **2** with fulvene **4**, we next focused on the aminocatalytic cycloaddition of formyl cycloheptatriene **1** with **4**. To our surprise, a [4 + 6] normal electron-demand cycloaddition followed by a 1,5-hydride shift in the cyclopentane core proceeds. Representative screening results are listed in Table 4.

Table 4. Screening of Aminocatalysts for the [4 + 6] Cycloaddition of Formyl Cycloheptatriene 1 with Fulvene 4

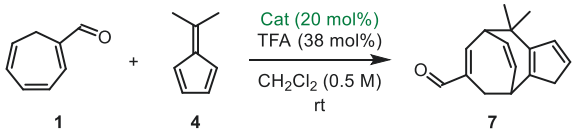

Entry	Catalyst	Time	NMR distribution [%][a] 1	7	ee [%][b]
1	**I**	7 d	57	12	–
2[c]	**I**	7 d	42	14	–
3	**I**	14 d	50	17 (11)	68
4[d]	**IX**	7 d	96	–	–
5[d]	**X**	22 d	87	–	–

[a]Determined by ^{1}H NMR analysis of the reaction mixture and relative to the internal standard 1,3,5-tris(trifluoromethyl)benzene. Isolated yield in parentheses. [b]ee measured by UPC^2. [c]At 40 °C. [d]With 19 mol % of TFA.

https://doi.org/10.1021/jacs.3c09551
J. Am. Chem. Soc. 2023, 145, 23874−23890

In contrast to the reaction between formyl cycloheptatriene **2** and fulvene **4**, the cycloaddition of formyl cycloheptatriene **1** was very sluggish, even at elevated temperatures. In the presence of (1*R*,2*R*)-1,2-diphenylethane-1,2-diamine **I** as the catalyst, the reaction proceeds as a [4 + 6] cycloaddition with the formation of the cycloadduct **7** in only 12% and 14% at room temperature and 40 °C, respectively, after a reaction time of 7 d (Table 4, entries 1 and 2). By increasing the reaction time to 14 days, only 11% of **7** was isolated with 68% ee (Table 4, entry 3). Changing the aminocatalyst to the naphthyl analogue of **I** did not significantly improve the yield and enantioselectivity (see Supporting Information Table S6). In line with the absence of reactivity of **2**, applying the common secondary aminocatalysts **IX** and **X**, the same lack of reactivity was observed for **1**.

Aminocatalytic Cycloaddition of Formyl Cycloheptatriene 3 with Fulvene 4. The aminocatalytic cycloaddition of formyl cycloheptatriene **3** with fulvene **4** also demonstrated a unique reactivity pattern. Here, a [4 + 2] inverse electron-demand cycloaddition proceeded via norcaradiene intermediate **N3**, affording cycloadduct **8**. For representative screening results, see Table 5.

Table 5. Screening of Aminocatalysts for the [4 + 2] Cycloaddition of Formyl Cycloheptatriene 3 with Fulvene 4

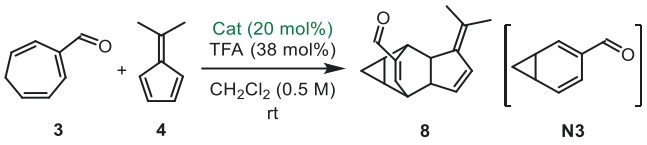

			NMR distribution [%][a]		
Entry	Catalyst	Time	3	8	ee [%][b]
1	**I**	7 d	17	48 (40)	68
2[c]	**I**	7 d	21	35 (34)	84
3[d]	**I**	7 d	94	–	–
4[e]	**IX**	7 d	100	–	–
5[e]	**X**	7 d	94	<1	–

[a]Determined by ^{1}H NMR analysis of the reaction mixture and relative to the internal standard 1,3,5-tris(trifluoromethyl)benzene. Isolated yield in parentheses. [b]ee measured by UPC^2. [c]With 38 mol % of TCA. [d]Without **4**. [e]With 19 mol % TFA.

Compared to formyl cycloheptatrienes **1** and **2**, formyl cycloheptatriene **3** demonstrated intermediate reactivity with fulvene **4** in the presence of (1*R*,2*R*)-1,2-diphenylethane-1,2-diamine **I** in CH_2Cl_2 with TFA as an additive. After a reaction time of 7 days, a significant proportion of **3** had been consumed along with the formation of 48% of the [4 + 2] cycloadduct **8**, which was isolated in 40% yield and 68% ee (Table 5, entry 1). The enantiomeric excess of **8** was improved to 84% ee by applying TCA as the additive; however, the reaction became more sluggish as exemplified by the lower conversion of 35% (Table 5, entry 2). It is likely that **3** and the norcaradiene intermediate **N3** are in a fast equilibrium.[63] ^{1}H NMR analysis of the reaction system without **4** did not reveal the formation of **N3** (Table 5, entry 3). We assume that **N3** is immediately trapped, in a [4 + 2] cycloaddition with **4**. For the organocatalytic cycloaddition of **3**, secondary aminocatalysts were incapable of bringing about any significant turnover at all (Table 5, entries 4 and 5), which also demonstrates the superiority of the diamine **I** to activate these polyenes through the formyl group.

Computational Investigations. As disclosed in Scheme 4 and the experimental results above, the reactivity of the formyl cycloheptatrienes is very dependent on the position of the formyl group. The experimental results show that formyl cycloheptatriene **1**, which is a linear conjugated system, reacts much more sluggishly compared to the formyl cycloheptatrienes **2** and **3**, which are cross-conjugated systems.

To explain the origins of the regioselectivity and the very unusual reaction patterns observed, coupled with the role of (1*R*,2*R*)-1,2-diphenylethane-1,2-diamine catalyst **I** in achieving the different cycloadditions, computational investigations were performed. The calculations were undertaken with DFT methods at the M06-2X/def2-TZVPP-CPCM(CH_2Cl_2)//M06-2X/def2-SVP-CPCM(CH_2Cl_2) level of theory.[64]

First, the calculations showed that **1**, with a linearly conjugated polyene system, is slightly more stable than **2** and **3** (Figure 1a). A similar situation also applies to the iminium ions, in which **1-Imin** is lower in energy than **2-Imin** and **3-Imin** by 1.6 and 0.8 kcal/mol, respectively (Figure 1b). The computed frontier molecular orbitals (FMOs) show that the aldehydes have relatively low-lying LUMOs, mainly localized on atoms C1, C2, C3, and C4 in **1**; C7, C1, C2, and C3 in **2**; and C1, C2, C3, and C4 in **3** (Figure 1a and Supporting Information Tables S8−S10). The fulvene has a relatively high-lying HOMO localized on Ca, Cb, Cc, and Cd (Figure 1c and Supporting Information Table S11). The calculations also showed that the formation of the imines from the aldehydes and the diamine catalyst is thermodynamically favored (Supporting Information Figure S5). The formation of an intramolecular hydrogen bond (Figure 1b, red dashed line) between the imine and the ammonium group of the catalyst contributes the most toward stabilizing the system (see Supporting Information Figure S6), but it has a limited effect on regioselectivity and reactivity; when the catalyst backbone is rotated to eliminate the intramolecular H-bonding, both the LUMO energy and the atomic orbital coefficients for the LUMO at the reacting carbons are almost unchanged (see Supporting Information Tables S8−S10). The iminium-ion species has a lower energy LUMO orbital than the aldehyde and thus should have enhanced reactivity (see Supporting Information Tables S8−S10). Upon iminium-ion formation, the LUMO distributions do not change significantly for **1-Imin** and **3-Imin**, compared to the cases of free aldehydes **1** and **3**. Importantly, the LUMO coefficients on atoms C2 and C3 of **2-Imin** are significantly lowered compared to **2**, and in the iminium-ion system, LUMO distributions will be significantly polarized toward the C7 position (Figure 1a,b and Supporting Information Tables S8−S10). A similar situation occurs for the norcaradiene isomers, but instead for the pair **N3** and **N3-Imin**, where the LUMO distributions will also be significantly polarized toward the C7 position (see Supporting Information Tables S12−S14).

For each formyl cycloheptatriene, the possibility of isomerization to its norcaradiene form was explored in the absence (Figure 2a,b) and presence of the aminocatalyst (Figure 2c,d). These calculations revealed that the valence isomerizations of the formyl cycloheptatrienes into bicyclic dienes are facile (**TS1**−**TS6**). The equilibrium of formyl cycloheptatriene with norcaradiene is rapid, and cycloadditions with fulvene are expected to proceed more slowly compared to the valence isomerizations. For the catalytic case, in addition to **TS4**−**TS6**, we also investigated the alternative transition states leading to the diastereomers. The computations indicate that for every instance, there is no preference toward either of the two diastereomers, and the competing transition states have almost the same energy (see Supporting Information Figure S7).

https://doi.org/10.1021/jacs.3c09551
J. Am. Chem. Soc. 2023, 145, 23874−23890

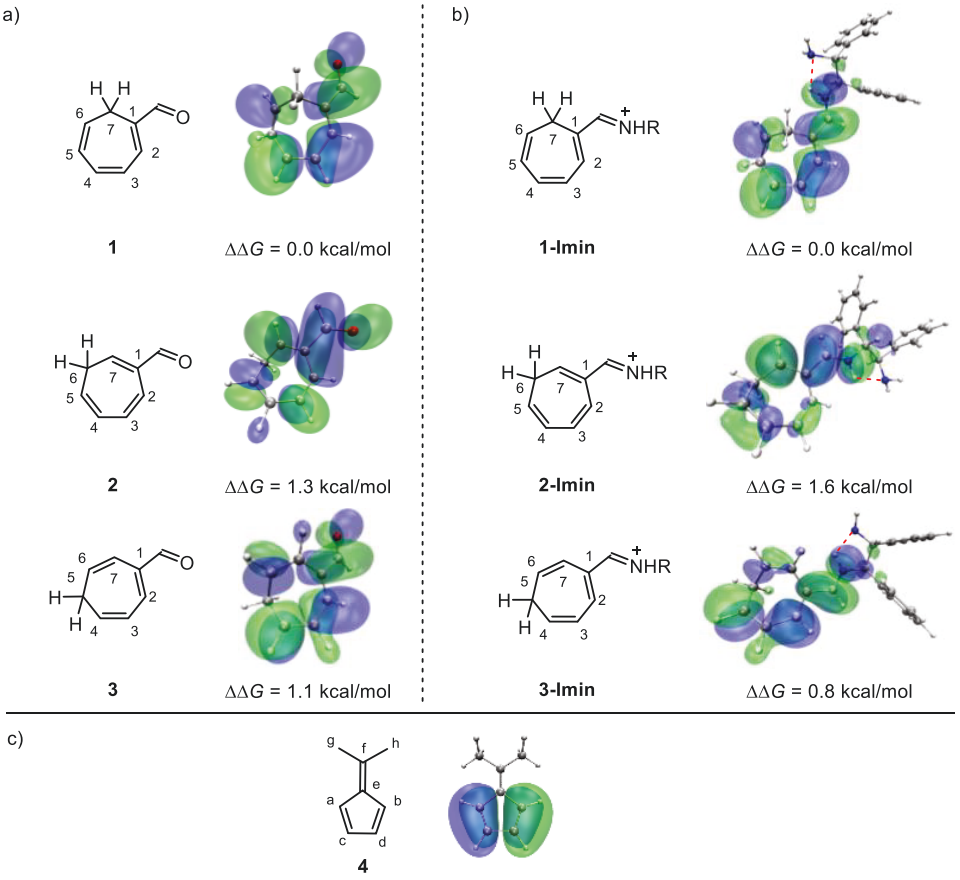

Figure 1. (a) LUMO orbitals of aldehydes, (b) iminium ions, and (c) HOMO orbital of **4**. For the noncatalytic case, free energies are compared to that of **1**. While for the catalytic case, free energies are compared to those of **1-Imin**. "*R*": "−CH(Ph)CH(Ph)NH_2" fragment in catalyst **I**.

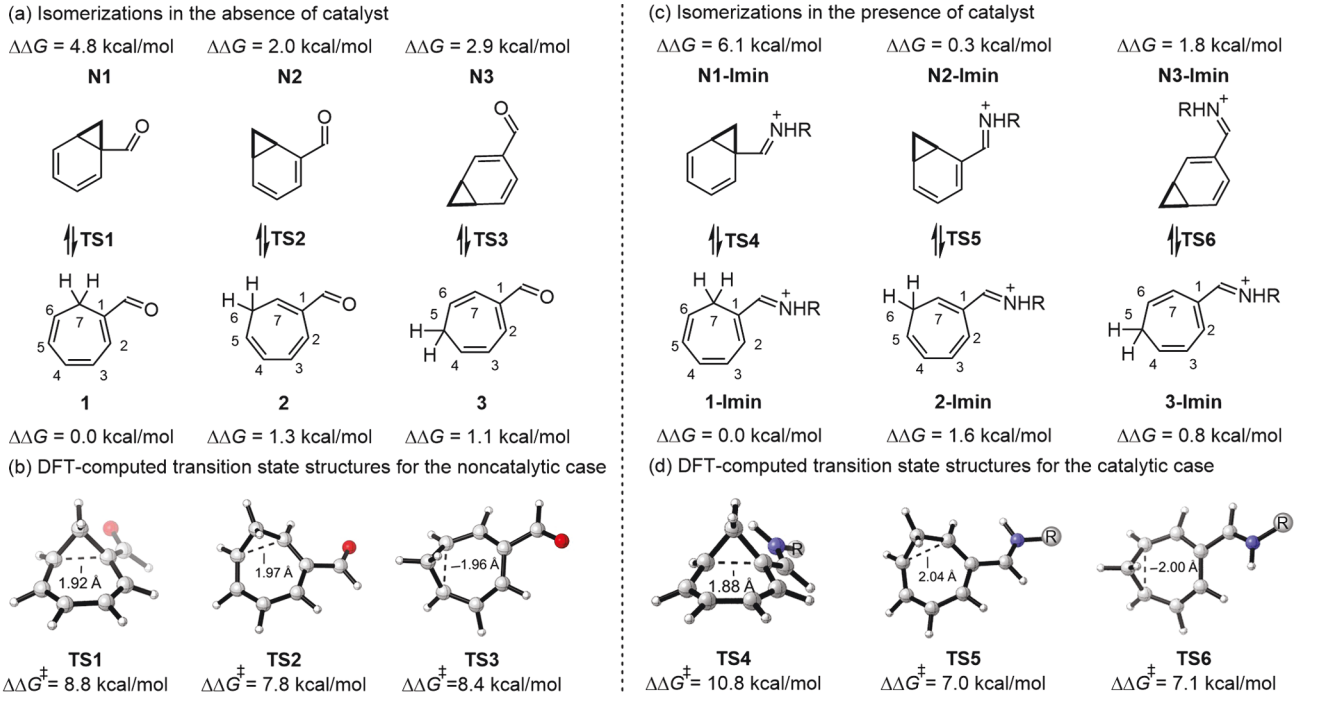

Figure 2. Isomerizations between formyl cycloheptatrienes **1**−**3** and norcaradienes under the noncatalytic (a and b) and catalytic (c and d) conditions. For the noncatalytic case, free energies are compared to that of **1**. For the catalytic case, free energies are compared to that of **1-Imin**.

For the noncatalytic case, formyl cycloheptatrienes (**1**−**3**) are more stable than the corresponding norcaradienes (**N1**−**N3**), and this phenomenon is also observed in the catalytic case for the reactions of **1-Imin** and **3-Imin**. In general, the cyclo-

https://doi.org/10.1021/jacs.3c09551
J. Am. Chem. Soc. 2023, 145, 23874−23890

heptatriene tautomer is thermodynamically more stable than the norcaradiene tautomer, which has a strained cyclopropane ring. Thus, the equilibrium lies on the side of the cycloheptatriene species, similar to several previous literature examples. However, the equilibrium between **2-Imin** and **N2-Imin** tends to favor the latter by 1.3 kcal/mol. This observation is related to the result of Ciganek[15] and others[65] where electron-withdrawing groups interact with and stabilize the Walsh occupied orbitals of the cyclopropane part of the norcardiene;[16] 7,7-dicyanocycloheptatriene is a stable norcaradiene. The interaction of a Walsh HOMO and an acceptor π^* orbital is shown schematically in Scheme 5. This is the well-established ability of cyclopropane

Scheme 5. Schematic Illustration of the Donor (Cyclopropane Walsh Orbital)−Acceptor (π^*-Orbital) Interaction

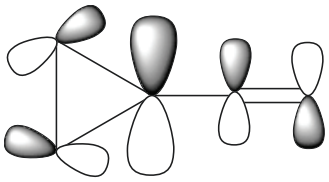

(donor) to enter into π-type conjugation with neighboring π-electron systems (acceptor). Similarly, we propose that in **N2-Imin**, the important stabilizing interaction is the mixing of an acceptor π^*-orbital of the substituted diene with an occupied Walsh orbital of the fused cyclopropane.[66−68] It should also be noted that **TS4** is 2.0 kcal/mol higher in energy than **TS1**, while both **TS5** and **TS6** are lower than **TS2** and **TS3**, with 0.8 and 1.3 kcal/mol, respectively. Thus, the aminocatalyst promotes the electrocyclization reaction of formyl cycloheptatrienes **2** and **3** but inhibits it for formyl cycloheptatriene **1**.

The reactions between fulvene **4** and the formyl cycloheptatrienes or their norcaradiene forms were explored for the [4 + 2], [4 + 6], or [6 + 2] pathways. In each instance, the following discussion will focus only on the most favorable pathway, although other approaches were also evaluated (see the Supporting Information).

The Formyl Cycloheptatriene 1 and Fulvene 4 System. The free energy changes of the most favorable pathway of the [4 + 6] cycloaddition of formyl cycloheptatriene **1** and fulvene **4** are shown in Figure 3 with aminocatalyst **I**. Iminium-ion formation (**1-Imin**) is thermodynamically favored by 1.6 kcal/mol. A subsequent cycloaddition occurs via a stepwise process in which the first C−C bond formation takes place via **TS7** with an energy barrier of 25.6 kcal/mol (**1-Imin** to **TS7**). **TS7** leads to intermediate **10**, which proceeds through **TS8** to generate the second C−C bond, leading to the formation of **11**. Cycloadduct **11** then undergoes a 1,5-hydrogen shift in the cyclopentadiene moiety, producing a stable intermediate **12**. Subsequent hydrolysis delivers the experimentally observed cycloadduct (**7**) and regenerates the active catalyst (**I**−**H**$^+$).

On the basis of the calculated free energy changes of the whole catalytic cycle, the on-cycle resting state is **1-Imin**, and the rate-determining step is the first C−C bond formation via **TS7** with an overall barrier of 25.6 kcal/mol. This energy barrier is feasible based on the experimental conditions (Table 4). The alternative transition state leading to the enantiomer of **7** (**7-*ent***) is higher in

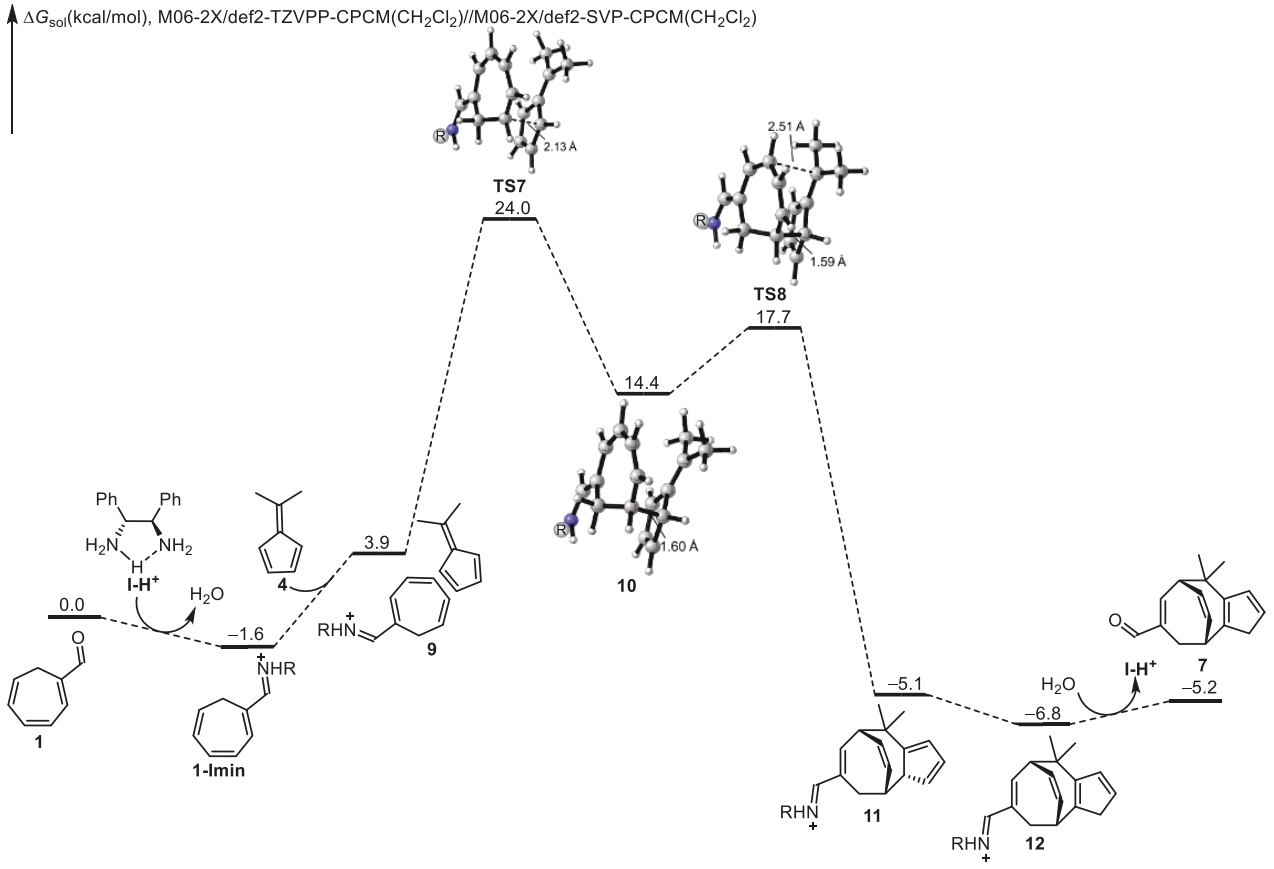

Figure 3. DFT-computed free energy changes of [4 + 6] cycloaddition of **1** and **4** under the aminocatalytic conditions.

https://doi.org/10.1021/jacs.3c09551
J. Am. Chem. Soc. 2023, 145, 23874−23890

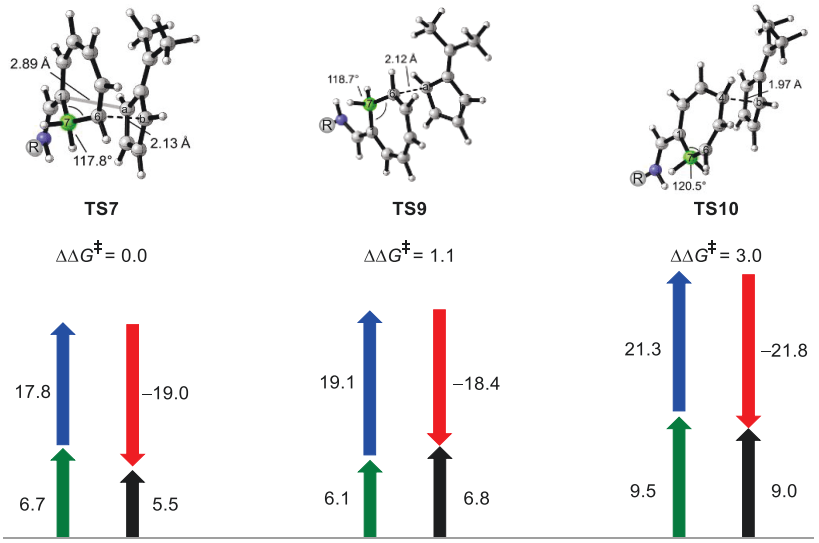

Figure 4. Distortion/interaction-activation strain (DIAS) analysis of the cycloaddition transition states to reveal the origins of regioselectivity for the cycloadditions of **1** and **4** under aminocatalytic conditions. Free energies were calculated at the M06-2X/def2-TZVPP-CPCM(CH_2Cl_2)//M06-2X/def2-SVP-CPCM(CH_2Cl_2) level of theory. Fragment distortion and interaction energies were calculated at the M06-2X level of theory with the def2-TZVPP basis set without the inclusion of solvation energy corrections (black, activation energies; blue, distortion energies of cycloheptatriene; green, distortion energies of fulvene; red, interaction energies). Energies are given in kcal/mol.

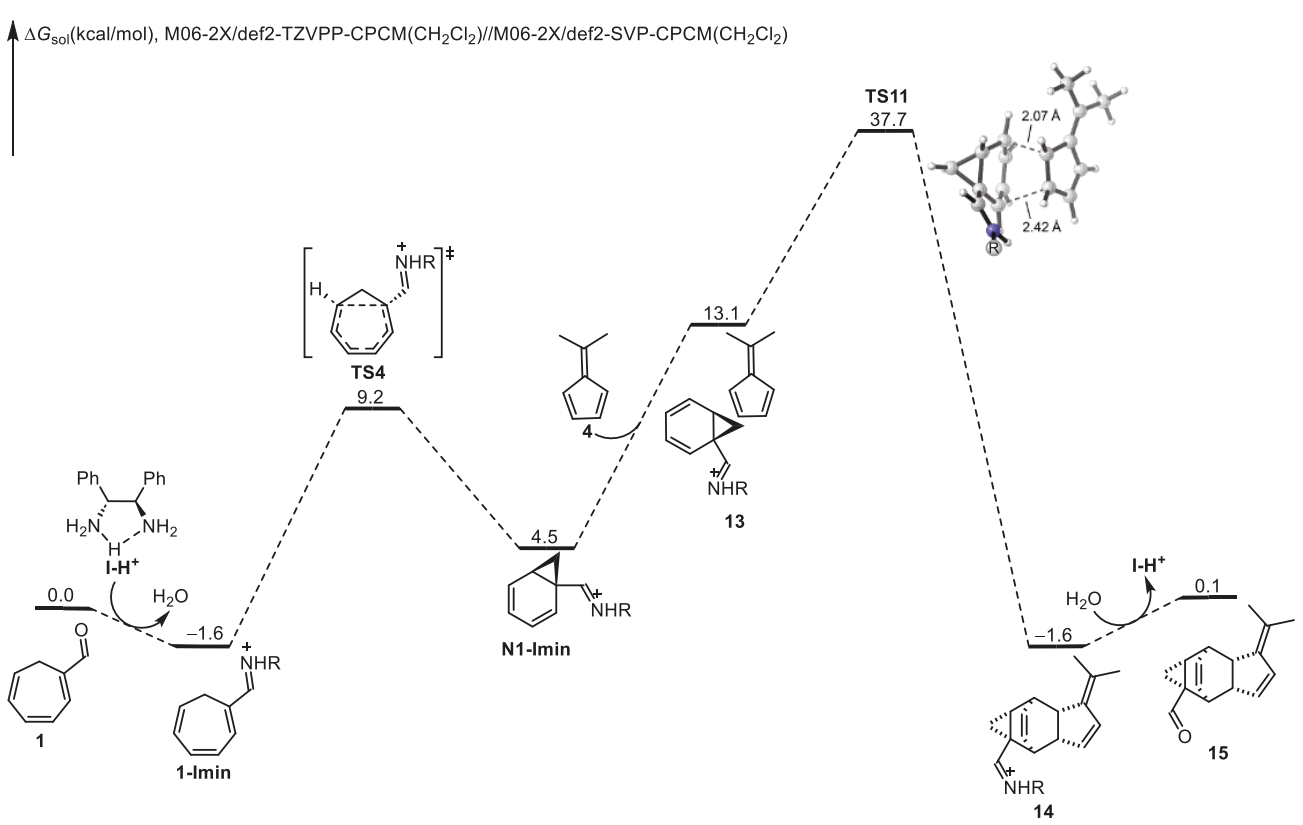

Figure 5. DFT-computed free energy changes of [4 + 2] cycloaddition of **1** and **4** with the involvement of **N1-Imin**, under the aminocatalytic conditions.

energy than **TS7** by 0.4 kcal/mol (see Supporting Information Figure S8), which is in line with the experimental enantiomeric excess (Table 4).

Reactions of formyl cycloheptatriene **1**, leading to [4 + 2] cycloadducts, were also investigated (see Supporting Information Figure S9). It can be envisioned that **1** can participate in a [4 + 2] cycloaddition as a 4π component through atoms C1−C4 (leading to **P1**) or C3−C6 (leading to **P2**). Under catalytic conditions, the envisioned [4 + 2] cycloadducts **P1** and **P2** would be obtained through stepwise transition states **TS10** and **TS9**, respectively (Figure 4). Both **TS9** and **TS10** are higher in energy than **TS7** by 1.1 and 3.0 kcal/mol in terms of Gibbs free energy (Figure 4).

https://doi.org/10.1021/jacs.3c09551
J. Am. Chem. Soc. 2023, 145, 23874−23890

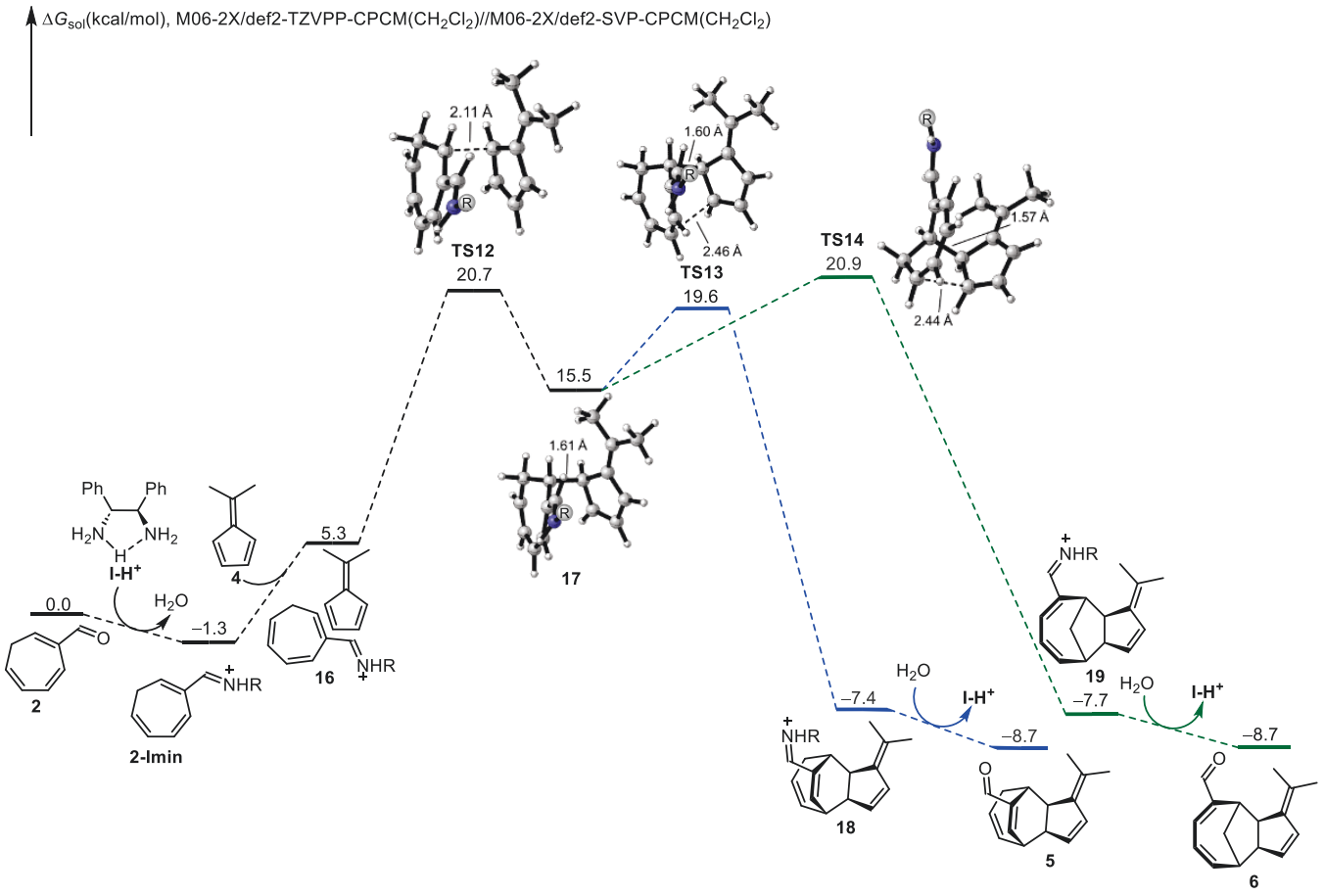

Figure 6. DFT-computed free energy changes of [4 + 2] or [6 + 2] cycloadditions of **2** and **4** under the aminocatalytic conditions.

Distortion-interaction analyses[69−74] were conducted to elucidate the origins of the regioselectivity for the cycloaddition event. As shown in Figure 4, **TS7** is 1.3 kcal/mol lower in energy compared to **TS9** in terms of electronic energy. The leading cause for this energy difference is distortion of the cycloheptatriene fragment, and it is greater in **TS9**. In **TS7**, there is a secondary orbital interaction between C1 and Ca (Figure 4), as indicated by the gray line (the C−C distance is 2.89 Å). However, this interaction is absent in **TS9**, and C1 is more engaged in conjugation between the imine system and the methylene moiety (C7) in the cycloheptatriene. Therefore, C7 of **TS9** tends to form sp^2-hybridization more than that of **TS7** due to conjugation (in **TS9**, the angle of ∠C1C7C6 is 118.7°, about 1° bigger compared to that of **TS7** (117.8°)), resulting in a large distortion of the cycloheptatriene fragment in the former (Figure 4). Transition state **TS10** is disfavored by 3.5 kcal/mol compared to **TS7** in terms of electronic energy. In **TS10**, the C−C bond forms to C4, while it forms to C6 in **TS7**. The atomic orbital coefficient of C4 is larger than that of C6 (see Supporting Information Table S8), resulting in a larger orbital interaction in **TS10**, but a later transition state. As a result, both cycloheptatriene and fulvene show significant distortions in **TS10**.[20] For example, in **TS10**, C7 is almost sp^2 hybridized (∠C1C7C6 = 120.5°). In short, **TS7** is the most favored transition state, leading to the observed cycloadduct.

Figure 5 shows the possible [4 + 2] cycloaddition arising from the norcaradiene tautomer. The cycloaddition occurs through a rate-determining concerted mechanism via **TS11**, and the overall barrier is 39.3 kcal/mol (**1-Imin** to **TS11**), almost as high as the noncatalytic process (see Supporting Information Figure S10). The reasons for this high energy barrier are that under catalytic conditions, (1) the valence isomerization from **1-Imin** to **N1-Imin** is thermodynamically disfavored by 6.1 kcal/mol, and most importantly, (2) in **N1-Imin**, the iminium fragment is no longer conjugated with the diene part of norcaradiene, so that the diene behaves like an ordinary, relatively unreactive, diene (see Supporting Information Tables S12−S14).

The Formyl Cycloheptatriene 2 and Fulvene 4 System. With aminocatalysis, the free energy changes of the most favorable pathway for the cycloaddition of **2** and **4**, leading to the experimentally observed cycloadducts, are shown in Figure 6. Starting from free aldehyde **2**, iminium formation (**2-Imin**) is thermodynamically favored by 1.3 kcal/mol. Subsequent cycloaddition occurs via a stepwise mechanism. The first C−C bond formation occurs through **TS12**. In **TS12**, the C−C bond forming distance is 2.11 Å, and it forms to C7 of the iminium component. This is consistent with the orbital distributions, in which the LUMO of the iminium ion is highly polarized toward C7, resulting in the most favored interaction at this position (Figure 1). **TS12** leads to a stepwise intermediate **17**, which can undergo either a [4 + 2] (via **TS13**) or a [6 + 2] (via **TS14**) cycloaddition to generate the second C−C bond, producing **18** and **19**, respectively (Figure 6). The final hydrolysis regenerates the active catalyst as well as the free cycloadduct (**5** or **6**). Other less favored pathways are included in the Supporting Information.

Since cycloadducts **5** and **6** have the same energy, the kinetic barrier determines the product distribution. The competition

https://doi.org/10.1021/jacs.3c09551
J. Am. Chem. Soc. 2023, 145, 23874−23890

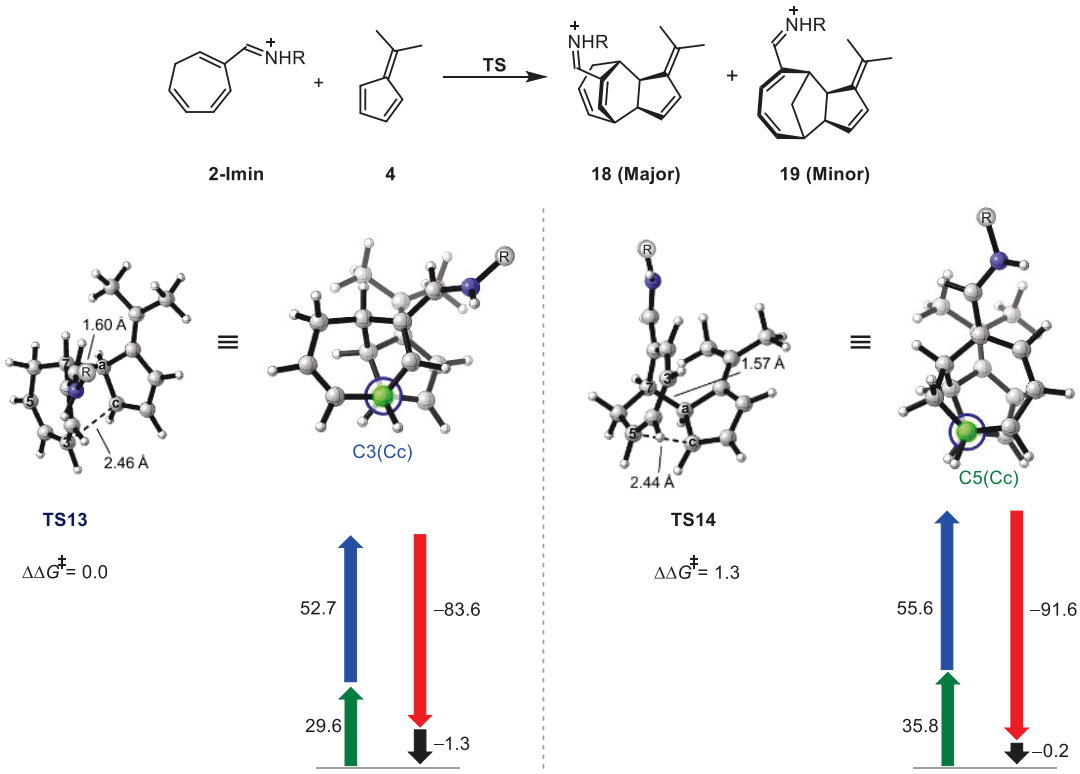

Figure 7. Distortion/interaction-activation strain (DIAS) analysis of the cycloaddition transition states to reveal the origins of regioselectivity for the cycloadditions of **2** and **4** under the aminocatalytic conditions. Energies are in kcal/mol. Legend is the same as that of Figure 4.

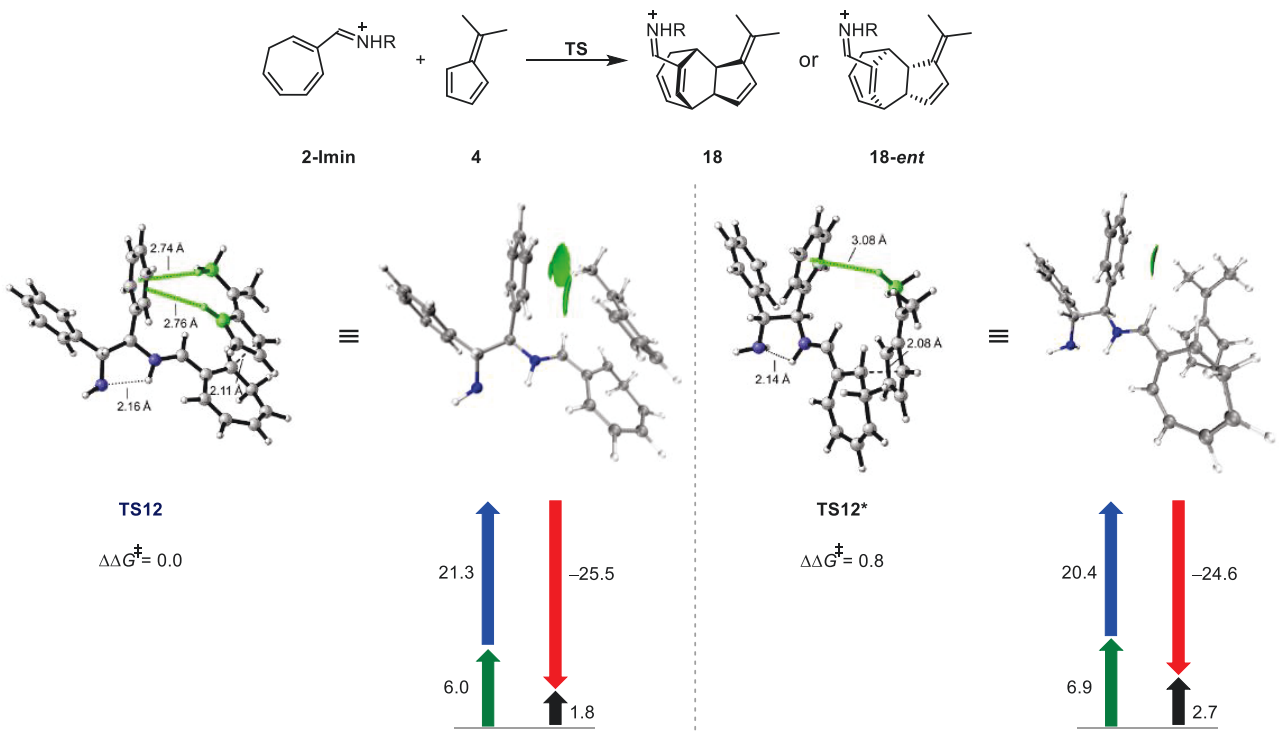

Figure 8. Distortion/interaction-activation strain (DIAS) analysis of the cycloaddition transition states to reveal the origins of enantioselectivity for the cycloadditions of **2** and **4** under the aminocatalytic conditions. Energies are in kcal/mol. Legend is the same as that of Figure 4.

between **TS13** (forming C3−Cc bond) and **TS14** (forming C5−Cc bond) determines the regioselectivity of the cycloaddition, as well as the product distributions. **TS13** is 1.3 kcal/mol lower in energy than **TS14** (roughly in line with the experimental observations). Cycloadduct **5** is the major adduct, and **6** is the minor one. Distortion-interaction analyses (Figure 7) indicate that the energy difference between **TS13** and **TS14** is brought about by the greater degree of substrates (both iminium and fulvene) distortions in **TS14** compared to **TS13**. This is facilitated by the fact that in order to form a C3−Cc bond, the

https://doi.org/10.1021/jacs.3c09551
J. Am. Chem. Soc. 2023, 145, 23874−23890

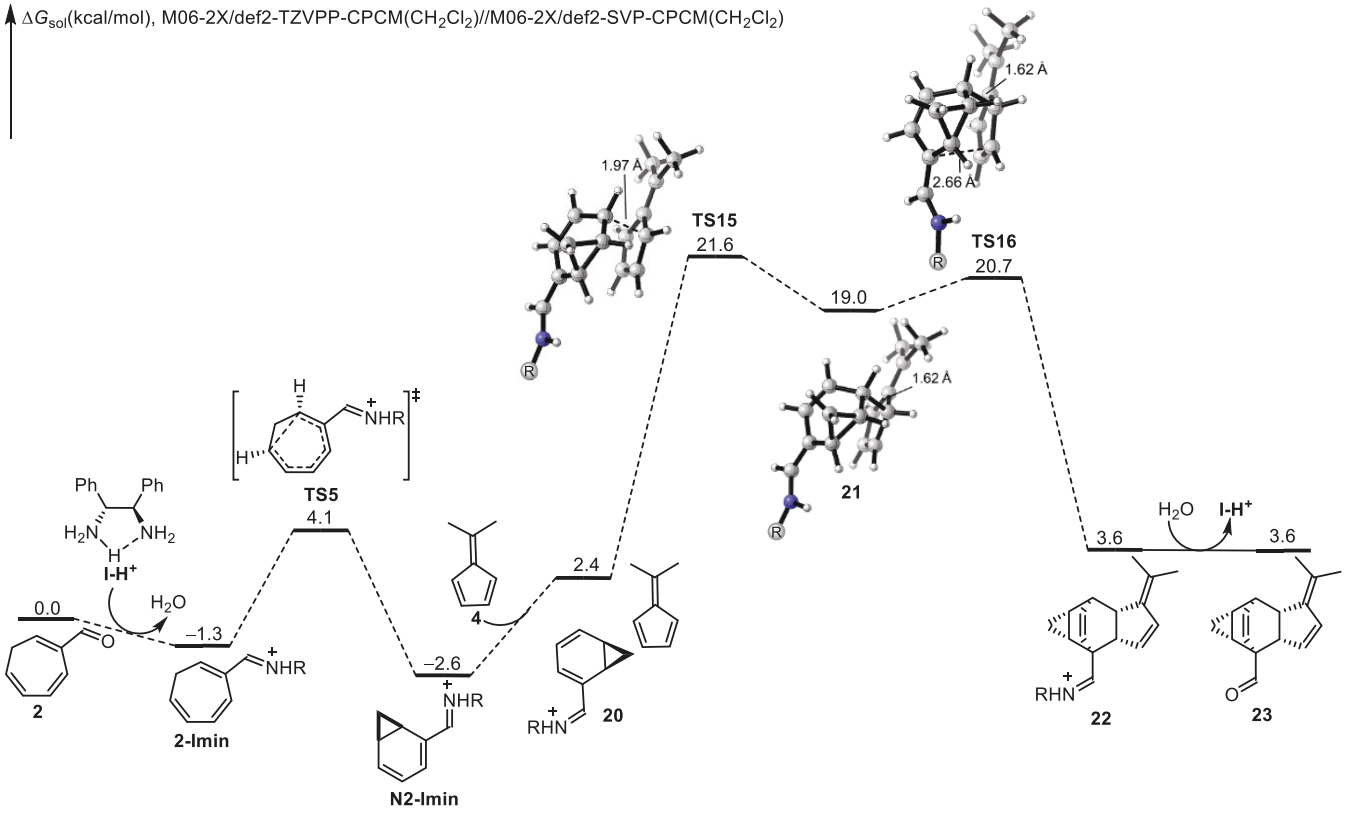

Figure 9. DFT-computed free energy changes of [4 + 2] cycloaddition of **2** and **4** with the involvement of **N2-Imin**, under aminocatalytic conditions.

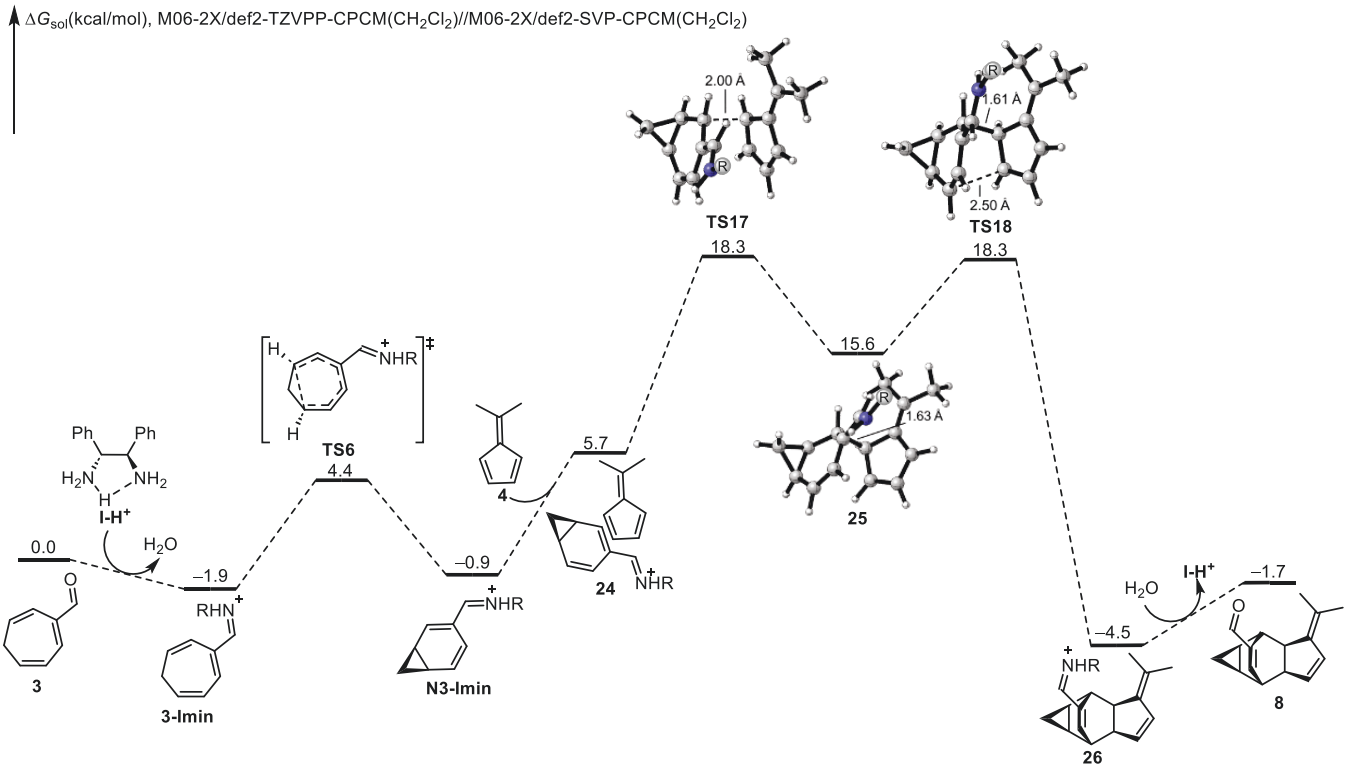

Figure 10. DFT-computed free energy changes of [4 + 2] cycloaddition of **3** and **4** with the involvement of **N3-Imin**, under aminocatalytic conditions.

substituents on the highlighted carbon atom (blue circle) in **TS13** can easily assume a staggered conformation with respect to the substituents of the carbon atom in the back of the Newman projection. In contrast, in the competing transition state **TS14**, the substituents around the forming C5−Cc bond almost eclipse each other (Figure 7), resulting in higher energy.

Regarding the formation of major cycloadduct **5**, the origins of the enantioselectivity were also investigated. As shown in Figure

https://doi.org/10.1021/jacs.3c09551
J. Am. Chem. Soc. 2023, 145, 23874−23890

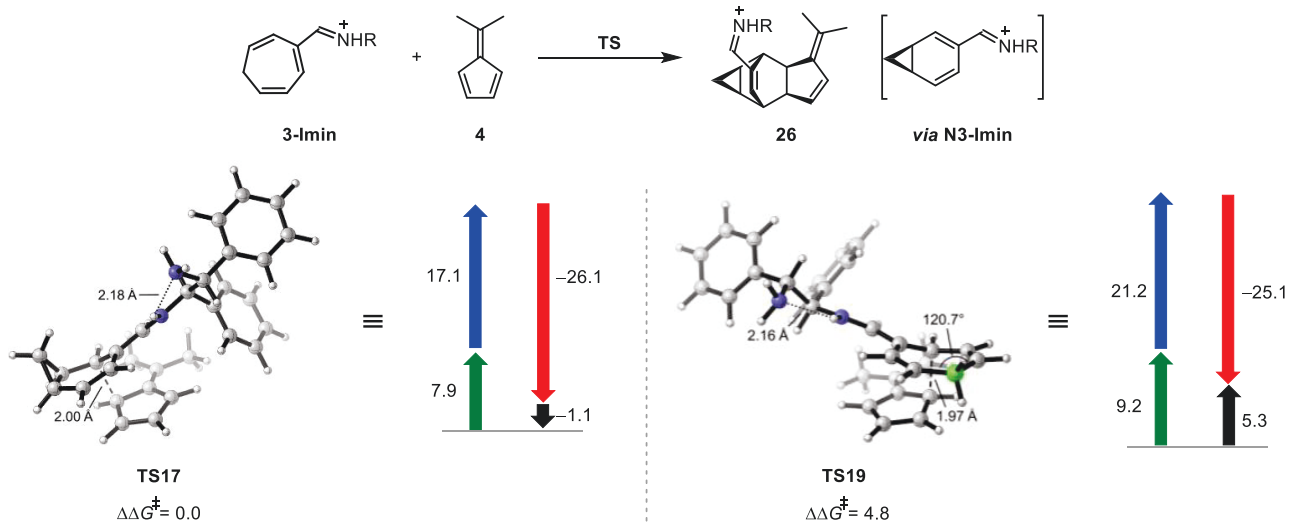

Figure 11. Distortion/interaction-activation strain (DIAS) analysis of the cycloaddition transition states to reveal the origins of chemoselectivity for the cycloadditions of **3** and **4** under the aminocatalytic conditions. Energies are in kcal/mol. Legend is the same as that of Figure 4.

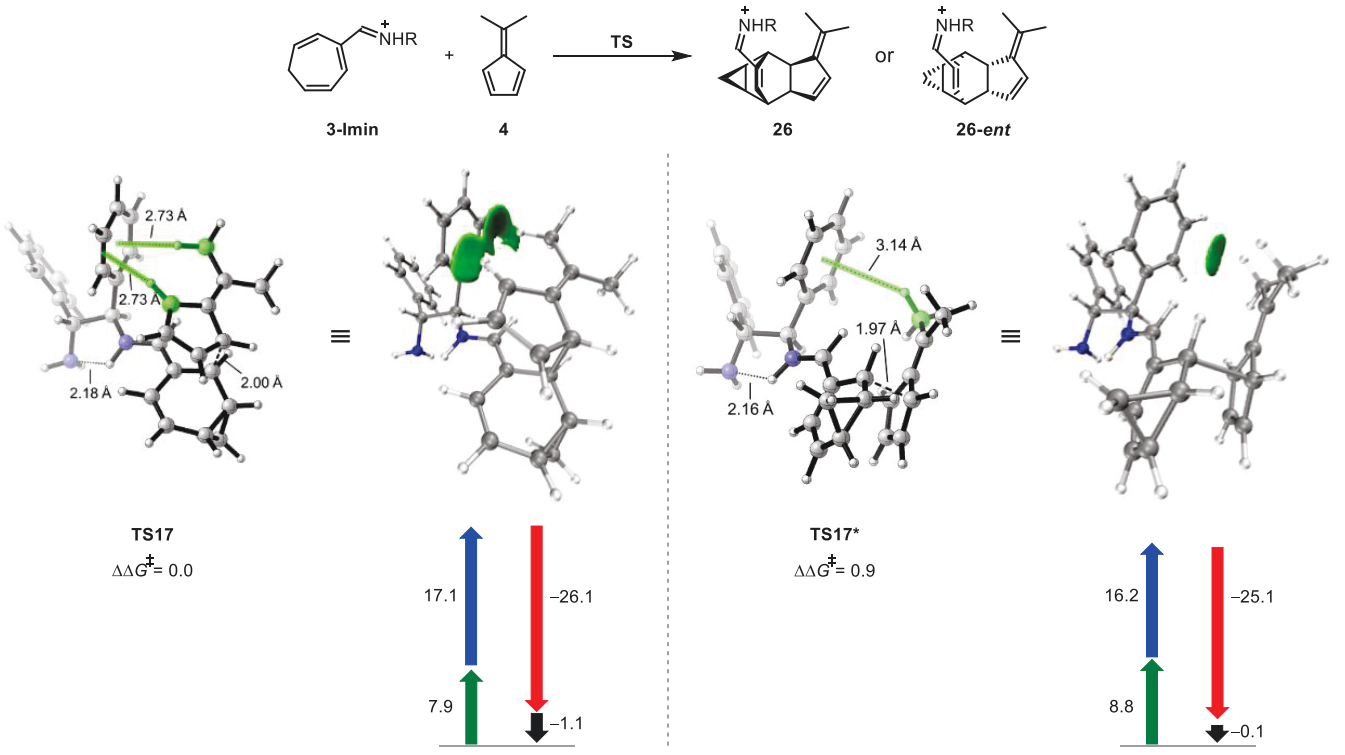

Figure 12. Distortion/interaction-activation strain (DIAS) analysis of the cycloaddition transition states to reveal the origins of enantioselectivity for the cycloadditions of **3** and **4** under the aminocatalytic conditions. Energies are in kcal/mol. Legend is the same as that of Figure 4.

8, **TS12** is 0.8 kcal/mol lower in energy than **TS12*** in terms of Gibbs free energy, leading to experimentally observed enantiomer **5**. DIAS analyses indicate that it is the interaction energy that controls the selectivity. Independent gradient model (IGM) analyses show that there are stronger CH−π interactions (between fulvene C−H bonds and phenyl group from the aminocatalyst) present in **TS12**, while they are weaker in **TS12***, eventually leading to the observed stereoselectivity. The distance of the CH−π interaction, 2.7−3.1 Å, is in the range of the dispersion effect. Since there is no discernible electrostatic interaction (see Supporting Information Table S15), dispersion is the main contributor to this observed noncovalent interaction.

Figure 9 shows the possible [4 + 2] cycloaddition arising from the norcaradiene isomer for the cycloaddition of **2** and **4** under catalytic conditions. The cycloaddition occurs through a stepwise mechanism. The rate-limiting first C−C bond formation occurs via **TS15**, and it leads to stepwise intermediate **21**, which proceeds through **TS16** to generate the second C−C bond formation product **22**. The overall barrier for cycloaddition via **TS15** is 24.2 kcal/mol (**N2-Imin** to **TS15**), and this barrier could be overcome at room temperature. This situation is very different from the case of **N1-Imin**, in which the cycloaddition via **TS11** (Figure 5) has a very high energy barrier. The main contributor for the enhanced reactivity of **N2-Imin** with fulvene is the conjugation between iminium and diene

https://doi.org/10.1021/jacs.3c09551
J. Am. Chem. Soc. 2023, 145, 23874−23890

fragments in the norcaradiene tautomer, lowering the LUMO energy of **N2-Imin** and facilitating the orbital interactions (see Supporting Information Table S13). As a result, **N2-Imin** acts as an activated diene (see Supporting Information Figure S13).

The cycloaddition through **TS15** is feasible in terms of Gibbs free energy, but the cycloadduct **23** (or **22**) is unstable, with an energy 3.6 kcal/mol higher than that of the free aldehyde **2** and 6.2 kcal/mol higher than that of the resting state **N2-Imin**. Compared to **N2-Imin**, both in **22** and **23**, the conjugation between iminium (or carbonyl) and olefin components no longer exists, thus making them higher in energy. Since the expected [4 + 2] cycloadduct **23** is thermodynamically disfavored, the cycloaddition is reversible, and the reaction actually occurs via the cycloheptatriene tautomer (Figure 6).

The Formyl Cycloheptatriene 3 and Fulvene 4 System. Under the aminocatalytic conditions, the free energy changes of the most favorable pathway for the cycloaddition of **3** and **4**, leading to the experimentally observed cycloadduct, are shown in Figure 10. Similar to previous cases (Figures 3, 5, 6, and 9), iminium-ion formation (**3-Imin**) is thermodynamically favored by 1.9 kcal/mol compared to the free aldehyde **3**. The following tautomerization generates **N3-Imin**, which then undergoes a stepwise mechanism to react with **4** through transition state **TS17** to form the first C−C bond. After that, intermediate **25** is formed, and this unstable intermediate further evolves into [4 + 2] cycloadduct **26** through **TS18**. The overall barrier for the cycloaddition event is 21.1 kcal/mol (**3-Imin** to **TS17**, then plus an additional 0.9 kcal/mol due to the catalyst regeneration). Once intermediate **26** is formed, the final hydrolysis regenerates the active catalyst (**I**−**H**$^+$) and delivers observed cycloadduct **8**.

Just like the cycloaddition of **N2-Imin** with fulvene, the reactivity of **N3-Imin** toward fulvene is higher due to the enhanced orbital interactions resulting from conjugation (see Supporting Information Table S14 and Figure S14). However, a notable difference between the **N2-Imin** case and the **N3-Imin** case is product stability. In the former case, the cycloadduct (Figure 9, **23**) is less stable due to the loss of conjugation. While in the latter case, the retained conjugation in **26** and **8**, makes the [4 + 2] cycloaddition shown in Figure 10 feasible thermodynamically.

The origins of the chemoselectivity for the aminocatalyzed cycloadditions of **3** and **4** were investigated. As shown in Figure 11, the competition between **TS17** and **TS19** determines the chemoselectivity, and the former is favored by 4.8 kcal/mol in terms of the Gibbs free energy, indicating that the product will be exclusively formed from the norcaradiene tautomer. DIAS analyses indicate that both distortion and interaction contribute to the selectivity. **TS17** is 1.0 kcal/mol more favored than **TS19** in terms of interaction energy, because the former has more favorable CH−π interaction between fulvene reactant and the phenyl group in the catalyst (Figure 12, green area in **TS17**). The major contributor to the energy difference of **TS17** and **TS19** is the distortion of the cycloheptatriene component, which is bigger in the latter than the former. In **TS19**, in order to accommodate the conjugation from iminium and olefin groups, the methylene moiety of cycloheptatriene needs to adopt a near-sp^2-hybridization (the highlighted bond angle is 120.7° in **TS19**, Figure 11), which is significantly different from its ground state, resulting in a large distortion. Other disfavored mechanisms resulting from the cycloheptatriene tautomer are included in the Supporting Information (Figures S15 and S16).

The origins of the enantioselectivity for the cycloaddition of **3** and **4** were also investigated through DIAS analyses. As shown in Figure 12, **TS17** is lower in energy than **TS17*** by 0.9 kcal/mol in terms of Gibbs free energy, leading to the preferred enantiomer. Fragment distortion and interaction analyses indicate that it is the interaction that controls the stereoselectivity. **TS17** has better interaction energy than **TS17***, due to the presence of stronger CH−π interaction (between fulvene C−H bonds and phenyl group from the aminocatalyst) in the former but smaller in the latter. The difference in the strength of the CH−π interaction can be seen from the IGM analysis (Figure 12). Since the bond lengths (2.7−3.1 Å) of the interacting CH−π are in the range of dispersion interaction, and no discernible electrostatic interaction is observed (see Supporting Information Table S16), we believe the dispersion interaction is the major factor leading to the enantioselectivity.

CONCLUSION

We have demonstrated that formyl cycloheptatrienes can undergo novel types of higher-order and classical cycloadditions dependent on the position of the formyl substituent relative to the cycloheptatriene core. These cycloadditions are made possible by applying a diamine catalyst capable of intramolecular hydrogen bonding, allowing for different activation modes of the formyl cycloheptatrienes reacting with 6,6-dimethylfulvene. The combination of this catalyst with cross-conjugated aldehydes made it possible to achieve the first enantioselective iminocatalytic inverse electron-demand [4 + 2] and [6 + 2] cycloadditions, affording the corresponding cycloadducts in up to 93% ee. Furthermore, an enantioselective iminocatalytic normal electron-demand [4 + 6] cycloaddition has been found to proceed for the linear-conjugated formyl cycloheptatriene. DFT-calculations were applied to provide insight into the unprecedented reactivity of the three different formyl cycloheptatrienes. These computational studies account for experimentally observed different reaction paths for the three isomeric formyl cycloheptatrienes; the major and minor reaction paths for the formyl cycloheptatrienes, where two cycloadducts are obtained, as well as for the observed enantioselectivities. The cycloadditions generally involve an attack of the most nucleophilic (largest HOMO coefficient) position of the fulvene on the most electrophilic site of the iminium-cycloheptatriene or iminium-norcaradiene. The computational investigations show that all of the catalytic cycloadditions proceed as stepwise reactions and can explain the observed experimental difference in reactivity between linear- and cross-conjugated systems. Importantly, single-conjugated systems (**2-Imin** and **N3-Imin**) are significantly more polarized toward the site of the first C−C bond formation (C7 position) compared to triple- (**1-Imin**) and double-conjugated systems (**3-Imin** which rearranges to the **N3-Imin**). These observations imply that cross-conjugated systems could offer interesting possibilities for the development of new cycloaddition reactions. Furthermore, conjugation also influences whether the cycloadduct is formed through the cycloheptatriene or the norcaradiene isomer. Thus, only formyl cycloheptatriene **3** gave a reaction through its norcaradiene isomer as conjugation between the formyl and diene fragment was preserved throughout the reaction. The peri- and chemoselectivity are calculated to be governed by minimizing the distortion of the transition state. On the other hand, the enantioselectivity is governed by maximizing dispersive interactions between the fulvene and diamine catalyst activated formyl cycloheptatriene.

https://doi.org/10.1021/jacs.3c09551
J. Am. Chem. Soc. 2023, 145, 23874−23890

■ ASSOCIATED CONTENT

Supporting Information

The Supporting Information is available free of charge at https://pubs.acs.org/doi/10.1021/jacs.3c09551.

Theoretical calculations, experimental procedures, characterization data, NMR spectra, UPCC chromatograms, and X-ray crystallographic data for the hydrazone derivative of **5** (PDF)

Accession Codes

CCDC 2168193 contains the supplementary crystallographic data for this paper. The data can be obtained free of charge via www.ccdc.cam.ac.uk/data_request/cif, or by emailing data_request@ccdc.cam.ac.uk, or by contacting The Cambridge Crystallographic Data Centre, 12 Union Road, Cambridge CB2 1EZ, UK; fax: + 44 1223 336033.

■ AUTHOR INFORMATION

Corresponding Authors

Karl Anker Jørgensen − *Department of Chemistry, Aarhus University, DK-8000 Aarhus C, Denmark;* orcid.org/0000-0002-3482-6236; Email: kaj@chem.au.dk

K. N. Houk − *Department of Chemistry and Biochemistry, University of California, Los Angeles, California 90095, United States;* orcid.org/0000-0002-8387-5261; Email: houk@chem.ucla.edu

Authors

Mikk Kaasik − *Department of Chemistry, Aarhus University, DK-8000 Aarhus C, Denmark*

Pan-Pan Chen − *Department of Chemistry and Biochemistry, University of California, Los Angeles, California 90095, United States;* orcid.org/0000-0002-3209-3841

Sebastijan Ričko − *Department of Chemistry, Aarhus University, DK-8000 Aarhus C, Denmark; Aarhus Institute of Advanced Studies, Aarhus University, DK-8000 Aarhus C, Denmark;* orcid.org/0000-0002-3013-3491

Complete contact information is available at: https://pubs.acs.org/10.1021/jacs.3c09551

Author Contributions

#M.K. and P.-P.C. contributed equally to this work.

Notes

The authors declare no competing financial interest.

■ ACKNOWLEDGMENTS

K.A.J. thanks Villum Investigator Grant (no. 25867), Novo Nordisk Foundation, FNU, and Aarhus University. K.N.H is grateful to the National Science Foundation (CHE-1764328 to K.N.H.) for financial support of this research. Calculations were performed on the IDRE Hoffman2 cluster at the University of California, Los Angeles. M.K. was supported by the Estonian Research Council grant (PUTJD1021). S.R. is supported by the European Union Horizon 2020 Research and Innovation Programme under the Marie Skłodowska-Curie Grant agreement number 754513 and by Aarhus University Research Foundation (AIAS-COFUND). Thanks are expressed to Dr. Mathias K. Thøgersen for X-ray analysis.

■ REFERENCES

(1) Curti, C.; Battistini, L.; Sartori, A.; Zanardi, F. New Developments of the Principle of Vinylogy as Applied to π-Extended Enolate-Type Donor Systems. *Chem. Rev.* **2020**, *120*, 2448−2612.

(2) Jessen, N. I.; McLeod, D.; Jørgensen, K. A. Higher-Order Cycloadditions in the Age of Catalysis. *Chem.* **2022**, *8*, 20−30.

(3) Nair, V.; Abhilash, K. G. [8 + 2] Cycloaddition Reactions in Organic Synthesis. *Synlett* **2008**, *2008*, 301−312.

(4) Frankowski, S.; Romaniszyn, M.; Skrzyńska, A.; Albrecht, Ł. The Game of Electrons: Organocatalytic Higher-Order Cycloadditions Involving Fulvene- and Tropone-Derived Systems. *Chem. Eur. J.* **2020**, *26*, 2120−2132.

(5) Battiste, M. A.; Pelphrey, P. M.; Wright, D. L. The Cycloaddition Strategy for the Synthesis of Natural Products Containing Carbocyclic Seven-Membered Rings. *Chem. Eur. J.* **2006**, *12*, 3438−3447.

(6) Nguyen, T. V.; Hartmann, J. M.; Enders, D. Recent Synthetic Strategies to Access Seven-Membered Carbocycles in Natural Product Synthesis. *Synthesis* **2013**, *45*, 845−873.

(7) Liu, N.; Song, W.; Schienebeck, C. M.; Zhang, M.; Tang, W. Synthesis of Naturally Occurring Tropones and Tropolones. *Tetrahedron* **2014**, *70*, 9281−9305.

(8) Takatsuki, K.; Murata, I.; Kitahara, Y. Thermal Dimerization of Tropilidene. *Bull. Chem. Soc. Jpn.* **1970**, *43*, 966−966.

(9) Caramella, P.; Quadrelli, P.; Toma, L. An Unexpected Bispericyclic Transition Structure Leading to 4 + 2 and 2 + 4 Cycloadducts in the Endo Dimerization of Cyclopentadiene. *J. Am. Chem. Soc.* **2002**, *124*, 1130−1131.

(10) Leach, A. G.; Goldstein, E.; Houk, K. N. A Cornucopia of Cycloadducts: Theoretical Predictions of the Mechanisms and Products of the Reactions of Cyclopentadiene with Cycloheptatriene. *J. Am. Chem. Soc.* **2003**, *125*, 8330−8339.

(11) Zhou, Q.; Thøgersen, M. K.; Rezayee, N. M.; Jørgensen, K. A.; Houk, K. N. Ambimodal Bispericyclic [6 + 4]/[4 + 6] Transition State Competes with Diradical Pathways in the Cycloheptatriene Dimerization: Dynamics and Experimental Characterization of Thermal Dimers. *J. Am. Chem. Soc.* **2022**, *144*, 22251−22261.

(12) D'Yakonov, V. A.; Kadikova, G. N.; Nasretdinov, R. N.; Dzhemileva, L. U.; Dzhemilev, U. M. The Synthesis of Bicyclo[4.2.1]-Nona-2,4,7-Trienes by [6π+ 2π]-Cycloaddition of 1-Substituted 1,3,5-Cycloheptatrienes Catalyzed by Titanium and Cobalt Complexes. *J. Org. Chem.* **2019**, *84*, 9058−9066.

(13) Ji, D.-W.; Hu, Y.-C.; Min, X.-T.; Liu, H.; Zhang, W.-S.; Li, Y.; Zhou, Y. J.; Chen, Q.-A. Skeleton-Reorganizing Coupling Reactions of Cycloheptatriene and Cycloalkenones with Amines. *Angew. Chem., Int. Ed.* **2023**, *62*, e202213074.

(14) Brember, A. R.; Freestone, V. C.; Gorman, A. A.; Sheridan, J. B. The Solution Photochemistry of Substituted Cycloheptatrienes. *Tetrahedron* **1979**, *35*, 2311−2322.

(15) Ciganek, E. The Direct Observation of a Norcaradiene-Cycloheptatriene Equilibrium. *J. Am. Chem. Soc.* **1965**, *87*, 1149−1150.

(16) Hoffmann, R. The Norcaradiene - Cycloheptatriene Equilibrium. *Tetrahedron Lett.* **1970**, *11*, 2907−2909.

(17) Matsumoto, M.; Shiono, T.; Kasuga, N. C. 7-Alkyl-7-Hydroxymethyl-3,4-Dimethoxynorcaradienes: A New Type of Norcaradiene Stabilized by π-Donors. *Tetrahedron Lett.* **1995**, *36*, 8817−8820.

(18) McNamara, O. A.; Maguire, A. R. The Norcaradiene-Cycloheptatriene Equilibrium. *Tetrahedron* **2011**, *67*, 9−40.

(19) Jansen, H.; Slootweg, J. C.; Lammertsma, K. Valence Isomerization of Cyclohepta-1,3,5-Triene and Its Heteroelement Analogues. *Beilstein J. Org. Chem.* **2011**, *7*, 1713−1721.

(20) Chen, P.-P.; Seeman, J. I.; Houk, K. N. Rolf Huisgen's Classic Studies of Cyclic Triene Diels-Alder Reactions Elaborated by Modern Computational Analysis. *Angew. Chem., Int. Ed.* **2020**, *59*, 12506−12519.

(21) Adam, W.; Balci, M.; Pietrzak, B. Reaction of 7-Substituted Cycloheptatrienes with Singlet Oxygen and 4-Phenyl-1,2,4-Triazoline-3,5-Dione. *J. Am. Chem. Soc.* **1979**, *101*, 6285−6291.

(22) Isakovic, L.; Ashenhurst, J. A.; Gleason, J. L. Application of Lewis Acid Catalyzed Tropone [6 + 4] Cycloadditions to the Synthesis of the Core of CP-225,917. *Org. Lett.* **2001**, *3*, 4189−4192.

(23) Okamura, H.; Iiji, H.; Hamada, T.; Iwagawa, T.; Furuno, H. Diels-Alder Reaction of α-Tropolone and Electron-Deficient Dienophiles Prompted by Et_3N or Silica Gel: A New Synthetic Method of

Highly Functionalized Homobarrelenone Derivatives. *Tetrahedron* **2009**, *65*, 10709−10714.
(24) Gritsch, P. J.; Gimenez-Nueno, I.; Wonilowicz, L.; Sarpong, R. Copper-Catalyzed [4 + 2] Cycloaddition of 9 *H*-Cyclohepta[*b*]-Pyridine-9-One and Electron-Rich Alkenes. *J. Org. Chem.* **2019**, *84*, 8717−8723.
(25) Zhang, H.; Thøgersen, M. K.; Jamieson, C. S.; Xue, X. S.; Jørgensen, K. A.; Houk, K. N. Ambimodal Transition States in Diels-Alder Cycloadditions of Tropolone and Tropolonate with *N*-Methylmaleimide. *Angew. Chem., Int. Ed.* **2021**, *60*, 24991−24996.
(26) Rigby, J. H.; Fleming, M. Construction of the Ingenane Core Using an Fe(III) or Ti(IV) Lewis Acid-Catalyzed Intramolecular [6 + 4] Cycloaddition. *Tetrahedron Lett.* **2002**, *43*, 8643−8646.
(27) Li, P.; Yamamoto, H. Lewis Acid Catalyzed Inverse-Electron-Demand Diels-Alder Reaction of Tropones. *J. Am. Chem. Soc.* **2009**, *131*, 16628−16629.
(28) Lauridsen, V. H.; Ibsen, L.; Blom, J.; Jørgensen, K. A. Asymmetric Brønsted Base Catalyzed and Directed [3 + 2] Cycloaddition of 2-Acyl Cycloheptatrienes with Azomethine Ylides. *Chem. Eur. J.* **2016**, *22*, 3259−3263.
(29) Hammer, N.; Erickson, J. D.; Lauridsen, V. H.; Jakobsen, J. B.; Hansen, B. K.; Jacobsen, K. M.; Poulsen, T. B.; Jørgensen, K. A. Catalytic Asymmetric [4 + 2]-Cycloadditions Using Tropolones: Developments, Scope, Transformations, and Bioactivity. *Angew. Chem., Int. Ed.* **2018**, *57*, 13216−13220.
(30) Bertuzzi, G.; McLeod, D.; Mohr, L.; Jørgensen, K. A. Organocatalytic Enantioselective 1,3-Dipolar [6 + 4] Cycloadditions of Tropone. *Chem. Eur. J.* **2020**, *26*, 15491−15496.
(31) Trost, B. M.; McDougall, P. J.; Hartmann, O.; Wathen, P. T. Asymmetric Synthesis of Bicyclo[4.3.1]Decadienes and Bicyclo[3.3.2]-Decadienes via [6 + 3] Trimethylenemethane Cycloaddition with Tropones. *J. Am. Chem. Soc.* **2008**, *130*, 14960−14961.
(32) Xie, M.; Liu, X.; Wu, X.; Cai, Y.; Lin, L.; Feng, X. Catalytic Asymmetric [8 + 2] Cycloaddition: Synthesis of Cycloheptatriene-Fused Pyrrole Derivatives. *Angew. Chem., Int. Ed.* **2013**, *52*, 5604−5607.
(33) Liu, H.; Wu, Y.; Zhao, Y.; Li, Z.; Zhang, L.; Yang, W.; Jiang, H.; Jing, C.; Yu, H.; Wang, B.; Xiao, Y.; Guo, H. Metal-Catalyzed [6 + 3] Cycloaddition of Tropone with Azomethine Ylides: A Practical Access to Piperidine-Fused Bicyclic Heterocycles. *J. Am. Chem. Soc.* **2014**, *136*, 2625−2629.
(34) Teng, H.-L.; Yao, L.; Wang, C.-J. Cu(I)-Catalyzed Regio- and Stereoselective [6 + 3] Cycloaddition of Azomethine Ylides with Tropone: An Efficient Asymmetric Access to Bridged Azabicyclo[4.3.1]Decadienes. *J. Am. Chem. Soc.* **2014**, *136*, 4075−4080.
(35) Mose, R.; Preegel, G.; Larsen, J.; Jakobsen, S.; Iversen, E. H.; Jørgensen, K. A. Organocatalytic Stereoselective [8 + 2] and [6 + 4] Cycloadditions. *Nat. Chem.* **2017**, *9*, 487−492.
(36) Wang, S.; Rodríguez-Escrich, C.; Pericàs, M. A. Catalytic Asymmetric [8 + 2] Annulation Reactions Promoted by a Recyclable Immobilized Isothiourea. *Angew. Chem., Int. Ed.* **2017**, *56*, 15068−15072.
(37) Gao, Z.; Wang, C.; Zhou, L.; Yuan, C.; Xiao, Y.; Guo, H. Phosphine-Catalyzed [8 + 2]-Annulation of Heptafulvenes with Allenoates and Its Asymmetric Variant: Construction of Bicyclo[5.3.0]-Decane Scaffold. *Org. Lett.* **2018**, *20*, 4302−4305.
(38) Wang, S.; Rodríguez-Escrich, C.; Fianchini, M.; Maseras, F.; Pericàs, M. A. Diastereodivergent Enantioselective [8 + 2] Annulation of Tropones and Enals Catalyzed by *N*-Heterocyclic Carbenes. *Org. Lett.* **2019**, *21*, 3187−3192.
(39) Frankowski, S.; Skrzyńska, A.; Albrecht, Ł. Inverting the Reactivity of Troponoid Systems in Enantioselective Higher-Order Cycloaddition. *Chem. Commun.* **2019**, *55*, 11675−11678.
(40) Yang, L. C.; Wang, Y. N.; Liu, R.; Luo, Y.; Ng, X. Q.; Yang, B.; Rong, Z. Q.; Lan, Y.; Shao, Z.; Zhao, Y. Stereoselective Access to [5.5.0] and [4.4.1] Bicyclic Compounds through Pd-Catalysed Divergent Higher-Order Cycloadditions. *Nat. Chem.* **2020**, *12*, 860−868.
(41) Melchiorre, P.; Marigo, M.; Carlone, A.; Bartoli, G. Asymmetric Aminocatalysis - Gold Rush in Organic Chemistry. *Angew. Chem., Int. Ed.* **2008**, *47*, 6138−6171.
(42) MacMillan, D. W. C. The Advent and Development of Organocatalysis. *Nature* **2008**, *455*, 304−308.
(43) Li, Q.-H.; Wei, L.; Wang, C.-J. Catalytic Asymmetric 1,3-Dipolar [3 + 6] Cycloaddition of Azomethine Ylides with 2-Acyl Cycloheptatrienes: Efficient Construction of Bridged Heterocycles Bearing Piperidine Moiety. *J. Am. Chem. Soc.* **2014**, *136*, 8685−8692.
(44) He, Z. L.; Sheong, F. K.; Li, Q. H.; Lin, Z.; Wang, C.-J. Exoselective 1,3-Dipolar [3 + 6] Cycloaddition of Azomethine Ylides with 2-Acylcycloheptatrienes: Stereoselectivity and Mechanistic Insight. *Org. Lett.* **2015**, *17*, 1365−1368.
(45) Sendra, J.; Salvado, O.; Pedrón, M.; Reyes, E.; Tejero, T.; Fernández, E.; Merino, P.; Vicario, J. L. Switchable Brønsted Acid-Catalyzed Ring Contraction of Cyclooctatetraene Oxide Towards the Enantioselective Synthesis of Cycloheptatrienyl-Substituted Homoallylic Alcohols and Oxaborinanes. *Adv. Synth. Catal.* **2023**, *365*, 1058−1071.
(46) Ahrendt, K. A.; Borths, C. J.; MacMillan, D. W. C. New Strategies for Organic Catalysis: The First Highly Enantioselective Organocatalytic Diels-Alder Reaction. *J. Am. Chem. Soc.* **2000**, *122*, 4243−4244.
(47) Erkkilä, A.; Majander, I.; Pihko, P. M. Iminium Catalysis. *Chem. Rev.* **2007**, *107*, 5416−5470.
(48) Moyano, A.; Rios, R. Asymmetric Organocatalytic Cyclization and Cycloaddition Reactions. *Chem. Rev.* **2011**, *111*, 4703−4832.
(49) Mukherjee, S.; Biswas, B. Organo-Cascade Catalysis: Application of Merged Iminium-Enamine Activation Technique and Related Cascade Reactivities. *ChemistrySelect* **2020**, *5*, 10704−10726.
(50) Jessen, N. I.; Bura, M.; Bertuzzi, G.; Jørgensen, K. A. Aminocatalytic [8 + 2] Cycloaddition Reactions toward Chiral Cyclazines. *Angew. Chem., Int. Ed.* **2021**, *60*, 18527−18531.
(51) Poulsen, P. H.; Vergura, S.; Monleón, A.; Jørgensen, D. K. B.; Jørgensen, K. A. Controlling Asymmetric Remote and Cascade 1,3-Dipolar Cycloaddition Reactions by Organocatalysis. *J. Am. Chem. Soc.* **2016**, *138*, 6412−6415.
(52) Gademann, K.; Chavez, D. E.; Jacobsen, E. N. Highly Enantioselective Inverse-Electron-Demand Hetero-Diels-Alder Reactions of α,β-Unsaturated Aldehydes. *Angew. Chem., Int. Ed.* **2002**, *41*, 3059−3061.
(53) Jiang, X.; Wang, R. Recent Developments in Catalytic Asymmetric Inverse-Electron-Demand Diels-Alder Reaction. *Chem. Rev.* **2013**, *113*, 5515−5546.
(54) Aga, M.; Okada, K.; Oda, M. Position and Dienophile Dependent Diels-Alder Reactions of Vinylcycloheptatrienes. *Tetrahedron Lett.* **1986**, *27*, 5653−5656.
(55) Buchi, G.; Burgess, E. M. Photochemical Reactions. X. 1,2 Experiments with 1,3,5-Cyclooctatrien-7-One and Cyclooctatetraene Epoxide. *J. Am. Chem. Soc.* **1962**, *84*, 3104−3109.
(56) Bornemann, C.; Klessinger, M. Excited-State Energy and Geometry Changes during the [1,7]H-Shift Reaction of Cycloheptatriene. *Org. Lett.* **1999**, *1*, 1889−1891.
(57) Steuhl, H.-M.; Bornemann, C.; Klessinger, M. The Mechanism of the Photochemical Hydrogen Migration in 1,3,5-Cycloheptatriene: A Theoretical Study. *Chem. Eur. J.* **1999**, *5*, 2404−2412.
(58) Ishihara, K.; Nakano, K. Design of an Organocatalyst for the Enantioselective Diels-Alder Reaction with α-Acyloxyacroleins. *J. Am. Chem. Soc.* **2005**, *127*, 10504−10505.
(59) Sakakura, A.; Suzuki, K.; Nakano, K.; Ishihara, K. Chiral 1,1′-Binaphthyl-2,2′-Diammonium Salt Catalysts for the Enantioselective Diels-Alder Reaction with α-Acyloxyacroleins. *Org. Lett.* **2006**, *8*, 2229−2232.
(60) Sakakura, A.; Suzuki, K.; Ishihara, K. Enantioselective Diels-Alder Reaction of α-Acyloxyacroleins Catalyzed by Chiral 1,1′-Binaphthyl-2,2′-Diammonium Salts. *Adv. Synth. Catal.* **2006**, *348*, 2457−2465.
(61) Kano, T.; Tanaka, Y.; Osawa, K.; Yurino, T.; Maruoka, K. Catalytic Enantioselective Construction of All-Carbon Quaternary Stereocenters by an Organocatalytic Diels-Alder Reaction of α-

https://doi.org/10.1021/jacs.3c09551
J. Am. Chem. Soc. 2023, 145, 23874−23890

Substituted α,β-Unsaturated Aldehydes. *Chem. Commun.* **2009**, 1956−1958.
(62) Eckert, F.; Leito, I.; Kaljurand, I.; Kütt, A.; Klamt, A.; Diedenhofen, M. Prediction of Acidity in Acetonitrile Solution with COSMO-RS. *J. Comput. Chem.* **2009**, *30*, 799−810.
(63) Balci, M.; Fischer, H.; Günther, H. The Dynamic Behavior of 2,4,6-Cycloheptatriene-1-Carbaldehyde. *Angew. Chem., Int. Ed.* **1980**, *19*, 301−302.
(64) Computational details are included in the Supporting Information.
(65) Bateman, L. M.; McNamara, O. A.; Buckley, N. R.; O'Leary, P.; Harrington, F.; Kelly, N.; O'Keeffe, S.; Stack, A.; O'Neill, S.; McCarthy, D. G.; Maguire, A. R. A Study of the Norcaradiene-Cycloheptatriene Equilibrium in a Series of Azulenones by NMR Spectroscopy; the Impact of Substitution on the Position of Equilibrium. *Org. Biomol. Chem.* **2015**, *13*, 11026−11038.
(66) Walsh, A. D. The Structures of Ethylene Oxide, Cyclopropane, and Related Molecules. *Trans. Faraday Soc.* **1949**, *45*, 179−190.
(67) Hoffmann, R. Some Theoretical Observations on Cyclopropane. *Tetrahedron Lett.* **1965**, *6*, 3819−3824.
(68) Hoffmann, R. Trimethylene and the Addition of Methylene to Ethylene. *J. Am. Chem. Soc.* **1968**, *90*, 1475−1485.
(69) Kitaura, K.; Morokuma, K. A New Energy Decomposition Scheme for Molecular Interactions within the Hartree-Fock Approximation. *Int. J. Quantum Chem.* **1976**, *10*, 325−340.
(70) Ziegler, T.; Rauk, A. A Theoretical Study of the Ethylene-Metal Bond in Complexes between Cu^+, Ag^+, Au^+, Pt^0, or Pt^{2+} and Ethylene, Based on the Hartree-Fock-Slater Transition-State Method. *Inorg. Chem.* **1979**, *18*, 1558−1565.
(71) van Leeuwen, P. W. N. M.; Kamer, P. C. J.; Reek, J. N. H.; Dierkes, P. Ligand Bite Angle Effects in Metal-Catalyzed C-C Bond Formation. *Chem. Rev.* **2000**, *100*, 2741−2770.
(72) van Zeist, W.-J.; Bickelhaupt, F. M. The Activation Strain Model of Chemical Reactivity. *Org. Biomol. Chem.* **2010**, *8*, 3118−3127.
(73) Fernández, I.; Bickelhaupt, F. M. The Activation Strain Model and Molecular Orbital Theory: Understanding and Designing Chemical Reactions. *Chem. Soc. Rev.* **2014**, *43*, 4953−4967.
(74) Bickelhaupt, F. M.; Houk, K. N. Analyzing Reaction Rates with the Distortion/Interaction-Activation Strain Model. *Angew. Chem., Int. Ed.* **2017**, *56*, 10070−10086.

https://doi.org/10.1021/jacs.3c09551
J. Am. Chem. Soc. 2023, 145, 23874−23890